Martina Marchetti-Deschmann

Master-Thesis

Systematic study of synthetic polymers by MALDI-linTOF-MS

submitted at TU Wien

Institute of Chemical Technologies and Analytics

under the supervision of

Associate Prof. Mag.rer.nat. Dr.rer.nat. Martina Marchetti-Deschmann

Univ.Prof. Dipl.-Ing. Dr.techn. Andreas Limbeck

by

Viktoria Untersulzner, BSc

Wien 2024, Viktoria Untersulzner

Acknowledgements

First of all, I would like to especially thank my thesis advisor, Martina Marchetti-Deschmann, for her guidance, help and constant support during the whole research work. I thank you for giving me the opportunity to conduct my master thesis in your group. I express my sincerest gratitude to the whole Research Group Mass Spectrometric Bio and Polymer Analysis for their friendship and support during my work at the institute. I thank Jakob Willner for his assistance with the experiments and the thorough discussions we had.

I also want to say thank you to my boyfriend for the help during the good and bad days. Thank you for always reminding me what is important and what not. Thank you also to my friends and family for the support and help during my studies.

"Live as if you were to die tomorrow. Learn as if you were to live forever."

— **Mahatma Gandhi**

Table of Contents

1 Abstract

Polymers find applications in many fields today. Still, their characterization and the determination of key characteristics, such as their monomer mass and molecular weight (MW) distribution, pose significant challenges. Mass spectrometry, with numerous techniques, is commonly employed for this purpose. Matrix assisted laser desorption/ionization linear time-of-flight mass spectrometry (MALDI-linTOF MS) allows the determination of monomer mass, molar mass, and end groups of a polymer.

The aim of this thesis was to develop a method allowing for the measurement of industrially relevant polymers. For this in a first step, sample preparation strategies for rather well-defined polymers were compared. Solid polyethylene glycol (PEG) samples with average molar masses of 400, 600, 1000,2,000 and 20,000 g/mol were dissolved in water/ethanol mixtures to form solutions with concentrations of 1, 0.5, and 0.25 mol/L. Various MALDI matrix at different concentration levels of 5, 10, and 20 g/mol were evaluated. Using the dried droplet method samples were prepared on a steel target. Additionally other industrial polymers with a wide range of masses were tested as polymer solutions, powders and thin films on a Si-Wafer using different MALDI matrices. One important goal of the theses was also the evaluation of MALDI-TOF MS as method to study polymer degradation. Polymer films were exposed to UV light, $SO_{2,g}$ and H_2S_g and subsequent measurements were compared to results from native polymers.

Each of the tested matrices proved suitable for measuring PEGs of different molecular masses. The structure and monomer mass could be confirmed. With these measurements the M_n (number-averaged MW) and M_w (weight-averaged MW) could be calculated, which yields information about the polydispersity of the PEGs.

MALDI-linTOF MS demonstrated effectiveness in measuring polymer films on a Si-Wafer. Polymer film degradation was observed. However, specific changes in polymer structure and the formation of characteristic mass differences have yet to be determined.

2 Deutsche Kurzfassung

Polymere finden heute Anwendungen in vielen Bereichen. Dennoch stellen ihre Charakterisierung und die Bestimmung wichtiger Eigenschaften wie ihrer Monomer-Masse und ihrer Molekülmasseverteilung (MW-Verteilung) erhebliche Herausforderungen dar. Die Massenspektrometrie wird mit zahlreichen Techniken häufig für diesen Zweck eingesetzt. Die Matrix-unterstützte Laser-Desorption/Ionisierung mit linearem Flugzeitmassenspektrometrie (MALDI-linTOF MS) ermöglicht die Bestimmung der Monomer-Masse, der Molmasse und der Endgruppen eines Polymers.

Das Ziel dieser Arbeit war die Entwicklung einer Methode zur Messung industriell relevanter Polymere. Dazu wurden zunächst verschiedene Strategien zur Probenvorbereitung für eher gut definierte Polymere verglichen. Feste Polyethylenglykol (PEG)-Proben mit durchschnittlichen molaren Massen von 400, 600, 1000, 2000 und 20.000 g/mol wurden in Wasser/Ethanol-Mischungen gelöst, um Lösungen mit Konzentrationen von 1, 0,5 und 0,25 mol/L zu bilden. Verschiedene MALDI-Matrixe bei verschiedenen Konzentrationen von 5, 10 und 20 g/mol wurden bewertet. Mit der Methode des getrockneten Tropfens wurden Proben auf einem Stahlziel vorbereitet. Zusätzlich wurden andere industrielle Polymere mit einem breiten Massenbereich als Polymerlösungen, Pulver und dünnen Filmen auf einem Si-Wafer unter Verwendung verschiedener MALDI-Matrixe getestet. Ein wichtiges Ziel der Arbeit war auch die Bewertung von MALDI-TOF MS als Methode zur Untersuchung von Polymerabbau. Polymerfilme wurden UV-Licht, SO_2 und H_2S ausgesetzt, und die nachfolgenden Messungen wurden mit Ergebnissen von nativen Polymeren verglichen.

Jede der getesteten Matrizen erwies sich als geeignet für die Messung von PEGs unterschiedlicher Molekülmassen. Die Struktur und die Monomer-Masse konnten bestätigt werden. Mit diesen Messungen konnten M_n (zahlengemittelte MW) und M_w (gewichtsgemittelte MW) berechnet werden, was Informationen über die Polydispersität der PEGs liefert.

MALDI-linTOF MS erwies sich als wirksam bei der Messung von Polymerfilmen auf einem Si-Wafer. Ein Abbau der Polymerfilme wurde beobachtet. Spezifische Veränderungen in der Polymerstruktur und die Bildung charakteristischer Massendifferenzen müssen jedoch noch bestimmt werden.

3 Abbreviations

PEG	Polyethylene glycol
UHQ	Ultra-high quality water without conducting ions
EtOH	Ethanol
ST	Stock solution
D1	Dilution 1
D2	Dilution 2
DHB	2,5-Dihydroxybenzoic acid
SA	Sinapinic acid
CHCA	α-Cyano-4-hydroxycinnamic acid
IAA	Indole-3-acetic acid
HABA	2-[(E)-(4-Hydroxyphenyl)diazenyl]benzoic acid
Norharman	9H-Pyrido[3,4-b]indol
DCTB	trans-2-[3-(4-tert-Butylphenyl)-2-methyl-2-propenyliden]-malonsäuredinitril
Harmaline	4,9-Dihydro-7-methoxy-1-methyl-3H-pyrido[3,4-b]indol
LP	Laser power
MW	Molecular weight
PVP	Polyvinylpyrrolidone
PMMA	Poly(methyl 2-methacrylate)
PI	Polyimide
PS	Polystyrene
PVA	Polyvinyl acetate
NaTFA	sodium trifluoroacetate
NaClO$_4$	sodium perchlorate/ iodide/ bromide/ chloride/TFA or AgTFA
AgTFA	silver trifluoroacetate
NaI	Sodium iodide
NaBr	Sodium bromide
NaCl	Sodium chloride
NaOAc	Sodium acetate
DMF	Dimethylformamide
MeOH	Methanol
Wt%	Weight percentage

4 Introduction and theory

4.1 Motivation

Over the course of the last century, polymers have come to be of ever greater importance. In today's world, polymers are used in many applications, ranging from everyday household items to sophisticated industrial and biomedical applications. The widespread utilization of polymers shows the importance of comprehensively understanding their structural properties, such as molecular weight distribution and monomer mass. These properties dictate a polymer's mechanical, thermal, and chemical characteristics, which in turn influence their performance and suitability for specific applications.[1]

As polymers continue to evolve with advancements in, for example, polymerization techniques, the precision in characterizing these structural properties becomes increasingly significant. This precision ensures the development of materials with tailored properties for specialized applications, thereby allowing progress in various sectors including automotive, aerospace and healthcare. [1, 2]

This thesis presents on one hand a general study on the applicability of matrix assisted laser desorption/ionization linear time-of-flight mass spectrometry (MALDI-linTOF MS) for the study of polymers and its potential to provide reproducible data for polymer characterization. Polyethylene glycol was systematically studied with different matrices, polymer masses and concentration ratios. On the other hand industrially relevant high molecular weight polymers of different structure and polarity were studied. Polymers relevant for coatings for electronics were chosen and assessed for potential degradation phenomena.

4.2 Matrix-assisted laser desorption/ionization

MALDI, an acronym for matrix-assisted laser desorption/ionization, represents a soft ionization technique within the field of analytical chemistry. This method is characterized by its ability to desorb/ionize analytes with minimal or no fragmentation. The process involves the utilization of a laser and an energy-absorbing matrix, specifically tailored to the wavelength in use.

In this technique, the laser imparts energy to the analyte molecules embedded in the matrix, leading to their ionization/desorption (Figure 1). Initially, a proton transfer occurs at the surface, followed by either desorption or gas-phase proton transfer within the resulting plume. This plume, formed from photoionized matrix molecules, serves as a medium for further ionization processes.

The ions generated in the gas phase undergo acceleration through an electrostatic field and are subsequently characterised within the analyser. This sequential process allows for the elucidation and examination of the molecular characteristics of the analyte ions. [3]
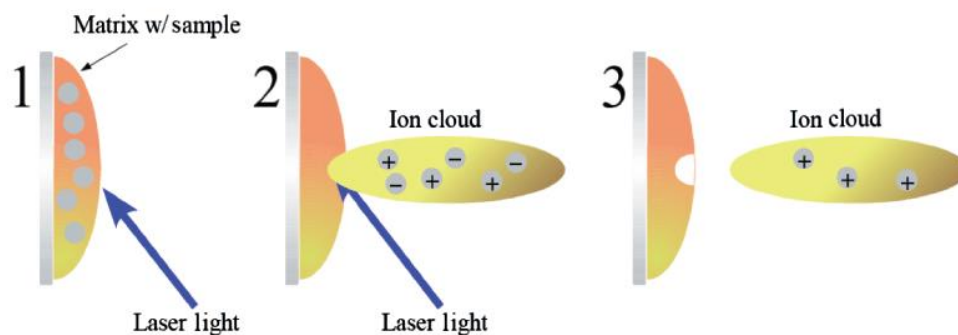
Figure 1: Schematic of the matrix-assisted laser desorption/ionization process. (1) The laser light is guided towards the sample surface and (2) produces a plume of ions that is (3) guided towards the mass analyser. (adapted from [4])

4.2.1 Light amplification by stimulated emission of radiation (laser)

The term "laser" originates from "Light Amplification by Stimulated Emission of Radiation". A laser produces monochromatic radiation that is characterized by linear polarization and high radiation intensity. Laser technology plays a pivotal role in MALDI, where distinctions can be made based on the laser's wavelength, leading to Ultra-Violet (UV) and Infrared (IR) MALDI variants. [3]

In UV-MALDI, the N_2 laser, operating at a wavelength of 337 nm, is the standard choice, along with the Nd:YAG laser emitting light at 355 nm. However, the N_2 laser presents challenges, including a limited pulse repetition frequency of <100 Hz and a finite number of emissions before replacement is required. The lower frequency can result in insufficient energy, diminishing the sensitivity of the measurements. A less common alternative is IR-MALDI, utilizing an Er:YAG laser with a wavelength of 2.94 µm. Minor variations in the spectra are discernible between these laser types. [3]

With IR lasers, a reduction in fragmentation is observed, accompanied by a diminished sensitivity. The reduced fragmentation in IR-MALDI is attributed to the lower temperature of the IR laser. However, this advantage comes at the cost of lower sensitivity, as the IR laser's different properties lead to more extensive vaporization of the sample with each laser shot, impacting the overall sensitivity of the analytical process. [5]

In UV-MALDI, the emission pulse duration varies between 0.5 ns and 25 ns, while in IR-MALDI, it ranges from 5 ns to 100 ns. The energy per pulse is relatively modest, with UV lasers requiring around 10-100 µJ, whereas IR lasers demand 100 µJ to 1 mJ. These parameters underscore the significance of selecting an appropriate laser system tailored to the specific requirements and objectives of the MALDI analysis. [5]

4.2.2 Matrix

The matrix plays an integral role in MALDI. It absorbs energy from the laser light and transfers it to the analyte, thereby minimizing damage caused by the laser pulse. The matrix serves as a protective barrier, absorbing a significant portion of the energy. The choice of matrix depends on the laser's wavelength and the nature of the analyte. Essential characteristics include low mass for sublimation, vacuum stability, and chemical inertness. [3]

Additional matrix requirements depend on the specific analyte. It should facilitate analyte ionization and be soluble in the same solvents as the analyte, ensuring similar polarity. Maintaining a sufficient matrix-to-analyte ratio is essential to prevent clustering in the gas phase. The clusters might falsely be measured as molecule ions, but more importantly can superimpose the actual mass spectrum of the sample giving less information for the analysis. The crystallisation behaviour of the matrix is equally important, since larger crystals can hinder analyte incorporation, potentially leading to mass spectra of low abundance. Smaller crystals have a higher surface area-to-volume ratio, allowing for increased contact of the surfaces of analyte and matrix. Consequently, smaller crystals enable a more rapid and complete transfer of energy from the matrix to the analyte [6].

The matrix significantly enhances the efficiency of energy transfer from the laser to the analyte. The transfer process becomes independent of the absorption properties and the size of the analyte, eliminating the need for wavelength adjustments when changing analytes. For instance, DHB with its 100 μm-sized crystals is ideal for protein analysis. The softness of DHB crystals prevents fragmentation, i.e. neutral loss, and peak tailing. Moreover, these crystals efficiently incorporate proteins while excluding common contaminants. [3] Table 1 gives an overview of different matrices and their typical field of applications.

Table 1: Commonly used matrices for UV-MALDI [5]

Analyte	Matrix	Abbreviation
Peptides/proteins	α-Cyano-4-hydroxycinnamic acid	CHCA
	2,5-Dihydroxybenzoic acid	DHB
	3,5 Dimethoxy-4-hydroxycinnaminic (Sinapic/sinapinic) acid	SA
Oligonucleotides	Trihydroxyacetophenone	THAP
	3- Hydroxypicolinic acid	HPA
Carbohydrates	2,5-Dihydroxybenzoic acid	DHB
	α-Cyano-4-hydroxycinnamic acid	CHCA
	Trihydroxyacetophenone	THAP
Synthetic polymers	Indole-3-acetic acid	IAA
	Dithranol	DIT
	2,5-Dihydroxybenzoic acid	DHB
Organic molecules	2,5-Dihydroxybenzoic acid	DHB
Inorganic molecules	Trans-2-(3-(4-tert-Butylphenyl)-2-methyl-2-propenyliedene]-malonnitrile	DCTB
Lipids	Dithranol	DIT

4.2.3 Sample preparation

The most common method for sample preparation in MALDI is the dried droplet technique. In this approach, the sample and matrix are dissolved either in the same solvent or in two miscible solvents. The matrix solution is typically saturated, while the sample solution has a lower concentration. The solvent mixture can be prepared before application on a steel target or directly on the sample support, often a stainless-steel target. The sample-to-matrix ratio, usually around 1:500, depends on the specific sample and matrix characteristics. The droplet that is applied on the target typically has a volume of 1 μL. It is either dried at room temperature, or under a flow of cold air, promoting the formation of sample/matrix

co-crystals. Depending on the solvent polarity, a high surface tension of the drop might lead to a non-homogeneous distribution of the crystals on the target. Manual intervention, active control, or the use of a crystal positioning/detection system for automated mass spectrometry measurements are therefore needed. Alternatively, the droplet can be dried under reduced pressure, or a more volatile solvent can be employed. Crucially, the crystallization of the matrix should remain rather consistent, even when dealing with small sample concentrations. [3]

Another method of sample preparation is the sandwich method. In this technique, a drop of matrix solution is applied to a spot, followed by the addition of a sample drop and another matrix drop. This method aims to enhance the incorporation of sample molecules into the matrix crystals. [7]

While there are alternative methods, they are less commonly used in this field due to inferior analyte incorporation into the matrix, resulting in lower mass resolution and/or sensitivity of measurement. For instance, the powder method involves mixing the sample and matrix as powder and pressing them onto the target. A significant challenge lies in ensuring that the particles are small enough to form a powder that can be effectively pressed together, creating a smooth surface to avoid diffuse reflection. [8]

4.2.4 Mass spectra characteristics

During the ionization process itself different ions are formed. This includes the combination of the molecular ion (M) with hydrogen (H), forming $[M+H]^+$ or $[M+2H]^{2+}$ or adducts with the matrix (m) or matrix fragments manifesting as $[M+m]^+$. Occasionally, sodium (Na) and potassium (K) ions form adducts ($[M+Na]^+$, $[M+K]^+$) with an additional 22 and 38 mass units, respectively, usually accompanied by a proton. These adducts, typically found near analyte peaks, can be identified based on their m/z values and the known species in the sample.

Fragmentation of the sample can happen during laser ablation in MALDI. Distinct types have been identified. In-source decay (ISD) occurs during the desorption ionisation process. From this, product ions are visible in the spectra, potentially at higher acceleration voltages. This type of fragmentation always appears in MALDI spectra. Prompt fragmentation occurs on or before the sample's surface during desorption, while fast fragmentation happens in the source, post-desorption but pre-acceleration. Post-source decay (PSD) follows during acceleration and occurs for metastable ions, resulting in peak broadening and subsequent loss of mass resolution and sensitivity. This type of fragmentation is not readily observed and requires specific instrumental conditions to be clearly identified. [5]

4.2.5 Mass analyser

To separate gas-phase ions based on their mass-to-charge ratios (m/z), various fields, including static, dynamic, or magnetic fields, alone or in combination, are employed. In the case of multiply charged ions, the apparent m/z represents only a fractional part of the actual mass. Key characteristics defining the performance of mass analysers include:

- Mass Range Limit: The m/z range covered by the mass analyser.
- Analysis Speed (Scan Speed): The rate at which the analyser measures over a specific mass range, typically expressed in units per second (u/s).
- Transmission: The ratio of the number of ions reaching the detector to the number of ions entering the mass analyser. This measure aims to account for ion loss.

- Mass Accuracy: The accuracy of the m/z provided by the mass analyser, representing the difference between the theoretical and the measured m/z (mmu/ppm). Mass accuracy is linked to the stability and resolution of the mass analyser.
- Resolution (Resolving Power): The observed m/z value divided by the smallest difference (Δ(m/z)) for two ions that can be separated. The resolution is high if the instrument can distinguish ions with a small mass difference.

Common mass analysers are Quadrupole, Ion trap, Time of Flight (TOF), Magnetic, Fourier Transform Ion Cyclotron Resonance (FTICR), and Orbitrap. [3, 5]

Time of flight analyser

After an initial acceleration step in an electrostatic field, ions undergo separation as they drift through a field-free region known as the flight tube. Ions are emitted from the source in bundles through two distinct processes. The first process is intermittent, resulting from plasma or laser desorption. The second process involves ion movement from the source upon the transient application of potential to the source. Once expelled from the source, ions experience acceleration towards the flight tube due to the potential difference between the electric and extraction grid. In this acceleration region, ions attain characteristic velocities, contingent upon their masses, as they all share the same kinetic energy. For details see Figure 2.
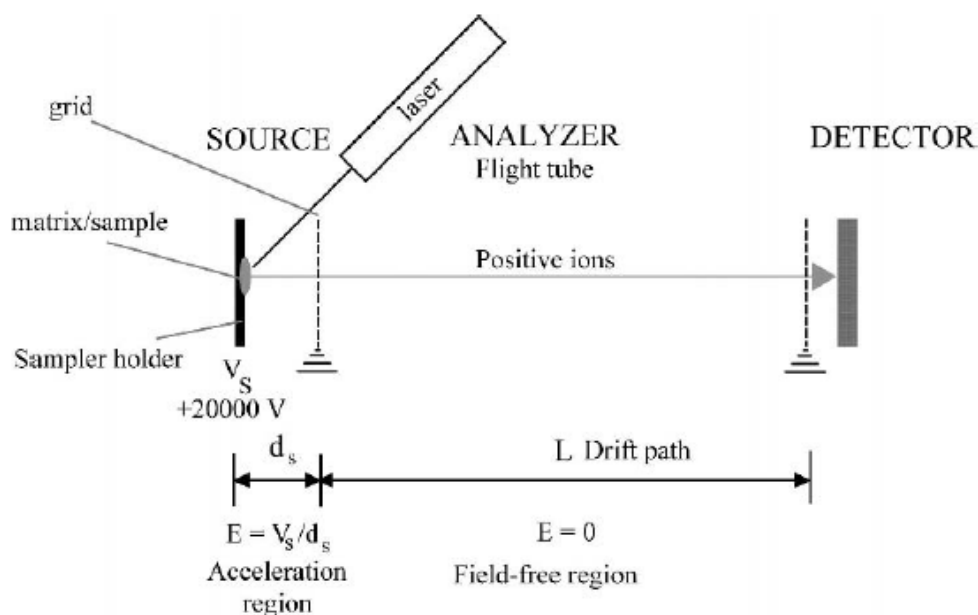
Figure 2: Principle of a linTOF [4]

Upon entering the field-free region, ions undergo separation based on their velocities, and the time taken by the ions to traverse this region and reach the detector is measured. This measurement can be expressed mathematically:

$$E_k = \frac{mv^2}{2} = qV_s = zeV_s = E_{el}$$

E_k...kinetic energy E_{el}...potential energy
V_s...potential   m...mass
v...velocity   q...charge =ze
z... charge number   e...electron charge

Upon rearranging Equation 1, the velocity can be calculated:

$$\frac{mv^2}{2} = zeV_s \rightarrow v = \left(\frac{2zeV_s}{m}\right)^{\frac{1}{2}}$$

Then the time t and the distance s replace the velocity v:

$$v^2 = \frac{s^2}{t^2} = \frac{2zeV_s}{m} \rightarrow t^2 = \frac{s^2 m}{2zeV_s}$$

$$t^2 = \frac{m}{z}\left(\frac{s^2}{2eV_s}\right)$$

Now Equation 4 is rearranged to calculate m/z.

$$\frac{t^2 2eV_s}{s^2} = \frac{m}{z}$$

Equation 5 shows the relationship between m/z and t^2. It illustrates that the smaller the mass of an ion, the faster it reaches the detector. This results in high transmission, leading to exceptional sensitivity and the ability to rapidly measure a broad mass range. A calibration equation is necessary to convert the observed physical property into a mass value, and both external and internal calibrations can be employed.

Equation 5 shows that the mass resolution is not only directly proportional to flight time but also indirectly proportional to the flight path length. Thus, lengthening the flight tube can increase the resolution. However, this may compromise performance. Increasing the flight tube length can lead to ion loss, attributed to scattering after collisions with other molecules or ions. Additionally, the angular dispersion of the ion beam causes ions to spread across a broader range of angles, further contributing to ion loss. Alternatively, the resolution can be enhanced by increasing the flight time by reducing the acceleration voltage. This approach diminishes the sensitivity.

The optimal combination for achieving the highest resolution and sensitivity involves using a flight tube of 1-2 meters in length and a 20 kV acceleration voltage. Further enhancements in resolution have been pursued through the development of two additional techniques: delayed pulsed extraction and reflectron.

For MALDI, TOF is the most commonly used mass analyser, because of its high mass resolution, fast scanning capabilities and suitability for analysing ions produced in the MALDI process. [3]

Delayed Pulsed Extraction

To mitigate peak broadening caused by ions with the same m/z ratio but varying kinetic energy, a time lag or delay between ion formation and extraction is implemented. This delay, ranging from 100 nanoseconds to one microsecond, allows ions to expand within the source. Subsequently, a voltage pulse is applied, extracting the ions from the source. During this delay, ions separate based on their kinetic energy. With the voltage pulse, additional energy is imparted to lower-energy ions before extraction, enabling them to catch up with higher-energy ions at the detector. This correction of energy dispersion among ions sharing the same m/z improves resolution. Achieving optimal results involves adjusting the focus pulse and delay independently, considering the mass of the analyte. For a given m/z and initial velocity distribution, a higher voltage pulse necessitates a shorter time delay, and vice versa. Consequently, optimization is specific to a portion of the mass range at a time, and its effectiveness diminishes at higher masses. [3]

Reflectron

The reflectron introduces a retarding field, functioning as a mirror that deflects ions. Typically, it comprises a series of electrodes or a ring electrode connected with a resistor. Positioned where the detector was originally located, the reflectron necessitates the relocation of the detector to the side of the source. The detector can be placed around the source or next to it, depending on whether the reflectron has a slight angle to deflect ions toward the detector off-axis.

The primary function of the reflectron is to correct the kinetic energy dispersion of ions with the same m/z. Ions with higher kinetic energy penetrate the reflectron more deeply, experiencing greater deceleration compared to ions with less kinetic energy. This correction enhances mass resolution by increasing the flight path without expanding the dimensions of the instrument. However, this improvement comes at the cost of sensitivity, leading to a reduced ability to measure lower concentrations of analyte. Furthermore, the enhanced mass resolution is limited to the optimized mass range. While a reflectron aids in better separation of post-source decay (PSD) fragments, providing more structural information, this advantage must be weighed against the drawbacks of peak broadening. [3]

4.3 Polymers

Polymers are molecules composed of repeating units (monomers) that are linked together. The structure of a polymer depends on its molecular bonds and monomer structure, which also has a significant impact on the properties. There are two major classes of polymers: natural and synthetic, distinguishing between human-made and naturally occurring polymers. Polymers can not only form chains but also other structures, including cyclic and branched configurations. The size and mass of the polymer can vary based on the number of repeating units, influencing characteristics such as the melting point or chain stability. This variability can be harnessed to tailor polymers for diverse applications. [9]

Polymers have frequently investigated by MALDI MS [10-13], carefully different types of polymers, using different matrices and sample preparation methods.

4.3.1 Characteristics of Polymers

Polymers can be characterised by defining their structure, composition, and properties. MALDI enables the determination of the molecular weight and structural information. For this purpose, parameters such as the repeating unit and the weight and number average molecular weights (M_w and M_n) are considered. The equations for calculating these are as follows:

$$M_w = \frac{\sum n_i M_i^2}{\sum n_i M_i}$$

<div align="right">Equation 6</div>

$$M_n = \frac{\sum n_i M_i}{\sum n_i}$$

<div align="right">Equation 7</div>
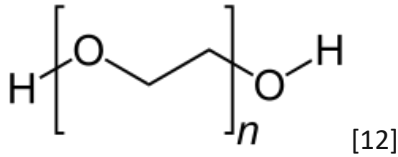
where n_i is the intensity and M_i is the m/z of the highest point of each peak. The polydispersity (PD) can be calculated using this information, providing insights into the molecular weight distribution (Equation 8). A higher PD indicates a broader distribution, with a greater variability in molecular weights within the sample. In contrast a lower PD indicates a narrower distribution with polymer chains with similar molecular weights. [10, 11]

$$PD = \frac{M_w}{M_n}$$

<div align="right">Equation 8</div>
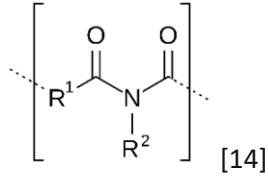
4.3.2 Polyethylene glycol

Polyethylene glycol (PEG) is a synthetic, hydrophilic, non-toxic, and biocompatible polymer. It is formed via a condensation reaction with ethylene oxide added to ethylene. It exhibits a linear structure. Below a molecular mass of 600, it is a liquid, while above 1000 it becomes solid. The polymer is soluble in water, alcohols, esters, ketones, aromatic solvents, and chlorinated hydrocarbons, but it does not dissolve in alkanes, paraffin, wax, and ether [12]. It finds applications in various fields, with common uses including drug delivery and surface functionalization such as coating, acting as a polar stationary phase for gas chromatography, and serving as an internal calibration compound in mass spectrometry. Additionally, it is an ingredient in many skin creams and lubricants, where it functions as a solubiliser and emulsifying agent [13].

Abbreviation	PEG
Chemical formula	$C_{2n}H_{4n+2}O_{n+1}$
Monomer structure	[12]
Monomer mass	44.05 g/mol
Polydispersity	Around 1.00
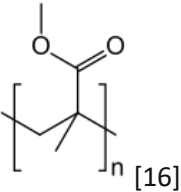
4.3.3 Polyimide

Polyimide (PI) is heat-resistant, chemical-resistant, and possesses a distinctive orange/yellow colour. It exhibits excellent dielectric properties and a low coefficient of thermal expansion. The most common method of synthesis involves a reaction between a dianhydride and a diamine or diisocyanate. Some common dianhydrides are pyromellitic dianhydride or benzophenone-3,3',4,4'-tetracarboxylic dianhydride (BTDA). For diamines, p-phenylenediamine (PPD) and 4,4'-oxydianiline (ODA) are often used [14]. This polymer finds application in insulating and passivating films, as coatings for optical fibers or microchips. When used as fibers, it can effectively filter hot gases, separating them from dust and particulate matter. By compressing the polymer powder into various shapes, it becomes suitable for use as mechanical parts in sockets and bearings or as medical tubing, owing to its high mechanical and temperature stability, and, in thin layers, its flexibility. The polymer is soluble in hot p-chlorophenol and m-cresol [15].

Abbreviation	PI
Chemical formula	$(R_1O_2NR_2)_n$
Monomer structure	[14]
Monomer mass	around 200 g/mol, depending on the $R^{1,2}$
Polydispersity	1.20-2.60
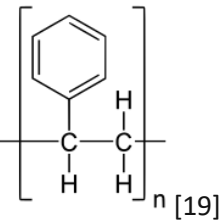
4.3.4 Polymethylmethacrylate

Polymethylmethacrylate (PMMA) is formed through radical polymerisation with methyl methacrylate. It can be employed as a glass substitute, owing to its high impact resistance and transparency [16]. Due to its compatibility with human tissue and non-toxic nature, it finds use in contact lenses, bone cement, and artificial teeth [17]. Its high resistance to UV light makes it suitable for use in tanning beds, acting as a barrier between the occupant and the bulbs. Additionally, it serves artistic and aesthetic purposes due to its durability and the ability to dye it in various colours that do not fade. The polymer is soluble in ethanol/water, ethanol/carbon tetrachloride, formic acid, and nitroethane [18].

Abbreviation	PMMA
Chemical formula	$(C_5O_2H_8)_n$
Monomer structure	[16]
Monomer mass	100.1 g/mol
Polydispersity	Around 1.00
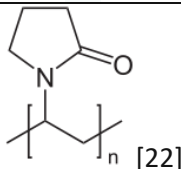
4.3.5 Polystyrene

Depending on its form, polystyrene (PS) can be utilized for various applications. In its solid or rigid state, it is transparent, brittle often employed for casings and housings. Its foam form is commonly used as insulation material or to produce food and drink containers [19]. Polystyrene films are found in take-out packaging for food and drinks, providing resistance against humidity. Due to its resistance to most acidic and basic chemicals, it is utilized in the medical and chemical fields for tubes and Petri dishes. However, it is soluble in many organic solvents such as benzene, tetrahydrofuran, and chloroform. Polystyrene is generally considered food-safe and non-toxic [20]. Being thermoplastic, it can be molded into different forms through temperature adjustment and additional polymerization of styrene, often achieved through vacuum processes [21].

Abbreviation	PS
Chemical formula	$(C_8H_8)_n$
Monomer structure	[19]
Monomer mass	104.2 g/mol
Polydispersity	1.02-3.50
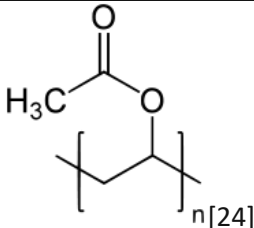
4.3.6 Polyvinylpyrrolidone

Polyvinylpyrrolidone (PVP) is formed from the monomer N-vinylpyrrolidone and is soluble in water and polar solvents, such as alcohols and amines. In its powdered form, it can absorb up to 40% of water. When dissolved, it forms films and exhibits excellent wetting properties, making it suitable for coating applications. This polymer is utilized in medicine as a binder for tablets, as it safely passes through the body, and is also employed in the production of contact lenses [22]. In the technical field, it serves as a stabilizing agent, emulsifier, and additive for batteries or ceramics. Additionally, it is found in personal care products like shampoo and hair gel, as well as a stabilizer in food [23].

Abbreviation	PVP
Chemical formula	$(C_6H_9NO)_n$
Monomer structure	[22]
Monomer mass	111.4 g/mol
Polydispersity	1.73-3.20

4.3.7 Polyvinyl acetate

Vinyl acetate reacts with oxygen, acetic acid, and free radicals to form polyvinyl acetate (PVAc). Due to the presence of an OH-group, it is hydrophilic and soluble in water. Its high polarity provides resistance to hydrocarbons, but it dissolves in alcohol-water mixtures, acetone, and chloroform, though not in pure alcohol [24]. It can be employed as a water dispersion for adhesive purposes in wood, paper, and cloth applications. The polymer is commonly used in envelope adhesives, gum bases for chewing gum, wallpaper adhesives, and bookbinding [25].

Abbreviation	PVA
Chemical formula	$(C_4H_6O_2)_n$
Monomer structure	[24]
Monomer mass	86.09 g/mol
Polydispersity	2.00

4.4 MALDI-linTOF Analysis of Polymers

In a MALDI measurement of a polymer with low molecular weight (below 10,000 Da), a distribution of peaks around the molecular mass of the polymer is observable. The difference between the peaks corresponds to the mass of the monomer. In Figure 3 polyethylene glycol is given as an example, with a molecular mass of 5,000 g/mol and a monomer mass of 44.05 g/mol (= 44 Da). Additionally, the mass of the repeating unit and the weight and number average molecular weights (M_w and M_n) and from that the polydispersity (PD or in this Figure D) can be calculated.
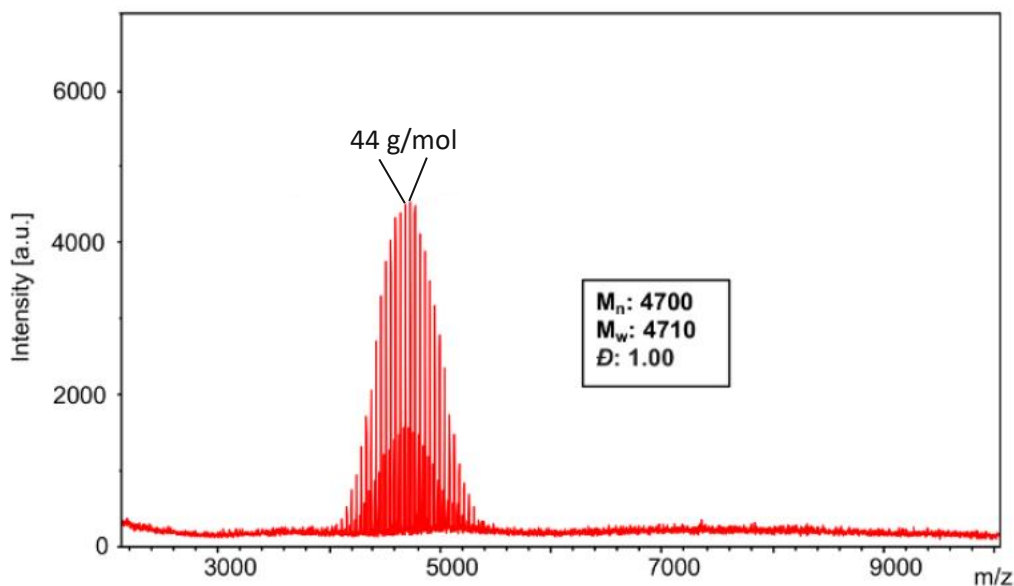
Figure 3: Polyethylene glycol in 2-aminoethyl acetic acid with M=5000 g/mol, adapted from [11]

For polymers with higher molecular weight (beyond 10,000 Da) mass resolution is usually not good enough to resolve the polymer distribution, making the determination of the monomers difficult. In Figure 4 Polymethylmethacrylate (PMMA) is shown with a molecular mass of (a) 6,100 g/mol and (b) 74,800 g/mol.
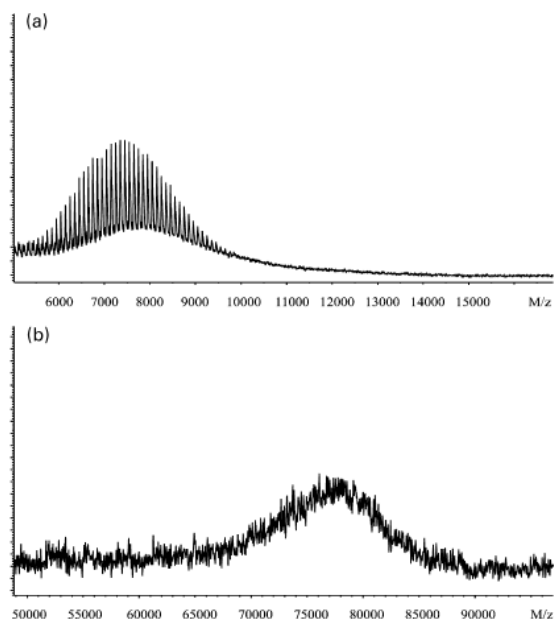
Figure 4: PMMA is shown with a molecular mass of (a) 6,100 g/mol prepared with sinapinic acid and (b) 74,800 g/mol prepared with indole-3-acetic acid as matrices [10]

5 Materials and Methods

5.1 Chemicals

In Table 2 all chemical reagents that were used throughout the course of this thesis are listed.

Table 2: Chemical reagents used in this thesis

Product	Company	Product Number	Note
Polyethylene glycol 400	Sigma-Aldrich	81284-1G	Analytical standard, for GCP
Polyethylene glycol 600	Sigma-Aldrich	81286-1G	Analytical standard, for GCP
Polyethylene glycol 1000	Merck	2890-1G	Certified reference material
Polyethylene glycol 2,000	Sigma-Aldrich		Analytical standard, for GCP
Polyethylene glycol 20.000	Sigma Aldrich	81298-1G	Analytical standard, for GCP
2,5-Dihydroxybenzoic acid	Aldrich	149357-100G	98%
3,5 Dimethoxy-4-hydroxycinnaminic (Sinapinic) acid	Aldrich	D7927-5G	≥98%, powder
α-Cyano-4-hydroxycinnamic acid	Sigma	C2020-25G	≥98% (TLC), powder
Indole-3-acetic acid	Sigma Aldrich		
2-[(E)-(4-Hydroxyphenyl)diazenyl]benzoic acid	Aldrich		
9H-Pyrido[3,4-b]indol	Sigma	N6252-100MG	crystalline
Trans-2-(3-(4-tert-Butylphenyl)-2-methyl-2-propenyliedene]-malonnitrile	Sigma-Aldrich	727881-1G	≥98%
4,9-Dihydro-7-methoxy-1-methyl-3H-pyrido[3,4-b]indol			
Methanol	Honeywell		LC-MS Chromasolv™ ≥99.9%
Tetrahydrofuran	Merck	8107	Dried, max. 0.01 H_2O for analysis
Ethanol	Honeywell	10193203	Chromasolv™, absolute, for HPLC, ≥99.8% (GC)
Polyvinylpyrrolidone	Provided by cooperation partner		No information
Poly(methyl 2-methacrylate)	Provided by cooperation partner		No information provided

Product	Company	Product Number	Note
Polyimide	Provided by cooperation partner		No information provided
Polystyrene	Provided by cooperation partner		No information provided
Polyvinyl acetate	Provided by cooperation partner		No information provided

5.2 Polyethylene glycol samples preparation

Five different polymer solutions were made from polyethylene glycol with molecular masses of 400, 600, 1000, 2,000 and 20,000 g/mol.
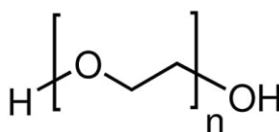
Figure 5: Polyethylene glycol [12]

The polymer was dissolved in a 1:1 mixture of ethanol (EtOH) and ultra high quality water (UHQ, with a conductivity of 18.2 MΩ·cm at 25°C) to achieve a concentration of 1 mg/mL, forming the stock solution (ST). Further dilutions were prepared to obtain 0.5 (D1) and 0.25 mg/mL (D2) solutions using the same solvent. The polymer masses and mixture volumes used for the preparation of the stock solutions is outlined in Table 3.

Table 3: Polymer masses and EtOH:UHQ 1:1 mixture volume used for the preparation of PEG stock solutions

Molar mass (g/mol)	Polymer mass (mg)	Mixture volume (mL)
PEG	PEG	EtOH:UHQ
400	0.9	0.9
600	1.0	1.0
1000	0.6	0.6
2,000	1.0	1.0
20,000	0.8	0.8

All used matrices, as well as their abbreviations, molar masses and used solvents are listed in Table 4. Three different solutions were made, with 5 mg/mL (5), 10 mg/mL (10) and 20 mg/mL (20) concentration.

Table 4: Matrix name with abbreviation, molar mass and used solvent

Matrix	Abbreviation	M (g/mol)	Solvent
2,5-Dihydroxybenzoic acid	DHB	154.03	EtOH
3,5 Dimethoxy-4-hydroxycinnaminic (Sinapinic) acid	SA	224.21	EtOH
α-Cyano-4-hydroxycinnamic acid	CHCA	189.17	EtOH
Indole-3-acetic acid	IAA	175.19	THF
2-[(E)-(4-Hydroxyphenyl)diazenyl]benzoic acid	HABA	242.23	THF
9H-Pyrido[3,4-b]indol	Norharman	168.19	THF
Trans-2-(3-(4-tert-Butylphenyl)-2-methyl-2-propenyliedene]-malonnitrile	DCTB	250.34	THF
4,9-Dihydro-7-methoxy-1-methyl-3H-pyrido[3,4-b]indol	Harmaline	214.27	THF

The sample preparation was carried out following the sandwich method, as described in Chapter 4.2.3 (sample preparation). First, 0.5 µL of matrix solution were applied on the target, followed by 0.5 µL of polymer solution, and then another 0.5 µL of matrix solution. In each row of the steel target, the matrix concentration varies, while in each column, the polymer molecular mass is changed (Figure 6). This was done for each of the matrices. Every sample was measured three times on different days with the same polymer solution and a new matrix solution every day and two times per laser power on the target spot.
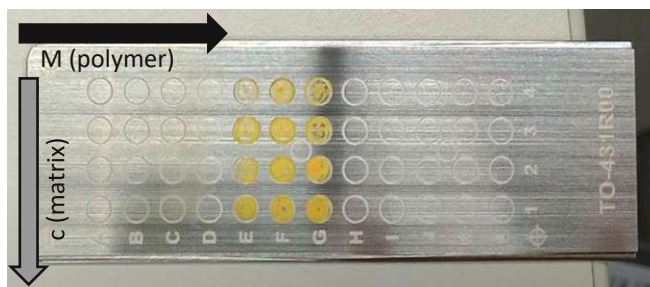
Figure 6: Steel target for MALDI-linTOF

For the comparison to the polymer films the cooperation partner made thin films from the PEG with a molecular weight of 2,000 and 20,000 g/mol. The exact procedure is not known, but two samples were provided each, with the only difference the curation temperature of 70°C and 120°C.

5.3 High molecular weight polymer samples preparation

Each polymer has different properties due to their completely different compositions, which depend on the monomer and the size of the polymer. Table 5 shows the polymer samples studied in this thesis.

Table 5: Polymers of interest for industrial application used in this study

Polymer	Abbreviation	Monomer	Monomer mass (g/mol)
Polyvinylpyrrolidone	PVP	$(C_6H_9NO)n$	111.14
Poly(methyl 2-methacrylate)	PMMA	$(C_5O_2H_8)n$	100.12
Polyimide	PI	$(R_1O_2NR_2)_n$	unknown
Polystyrene	PS	$(C_8H_8)n$	104.15
Polyvinyl acetate	PVA	$(C_4H_6O_2)n$	86.09

All polymers are very different with respect to physicochemical properties and therefore require different matrices, solvents, and instrument settings. The available literature provides options, that have already been tested and the selection is listed in Table 6.

Table 6: Sample preparation strategies for high molecular weight polymers [26]

Polymer	Recipe	Matrix	Salt	Solvent
PVP	1	DHB		water, acetonitrile
	2	IAA	NaTFA	MeOH
PMMA	1	DHB	NaClO4/NaI/ NaBr/NaCl/NaTFA or AgTFA	THF
	2	IAA	AgTFA	THF/ chloroform or acetone
	3	DCTB	NaTFA/NaI	THF
	4	CHCA	NaI	THF/water
	5	dithranol	NaOAc	2-propanol/MeOH, chloroform
PI	1	DHB	NaI	DMF
	2	dithranol	NaI in methanol	DMF/THF
PS	1	DCTB	KI	MeOH
	2	CHCA	NaI, NaTFA, AgTFA	THF
	3	IAA		THF
	4	HABA		THF
	5	dithranol	AgTFA	THF
PVA	1	DHB	LiBr	MeOH
	2	IAA	LiBr	MeOH
	3	DCTB	LiBr	MeOH

Only a selection of three different sample preparation strategies were tested. The selection was based on the following rational: (a) solubility of polymers in the different solvent and (b) the application of the matrix to thin polymer films.

Polymer solutions

Samples prepared in N-methyl-pyrrolidone (NMP) with concentrations expressed as polymer weight percentage (Wt%) in the solvent were used (Table 6).

Table 7: Weight percentages and provided molecular weights of the polymers

Polymer	Wt%	Presumed molecular mass (g/mol)
PVP	8	1,300,000
PMMA	15	35,000
PI	10	unknown
PS	20	800-5,000
PVA	15	unknown

PVP was excluded from the experiments. Although the molecular mass is within the mass range for a MALDI linTOF experiment [27], the measurement of polymers is significantly hampered by the increasingly apolar character of the analyte. The following matrices were used for the measurements: DHB, SA, CHCA, HABA, and IAA. Each of the matrices was dissolved in THF (10 mg/mL). To achieve solutions with the same polymer concentrations the polymer solutions were diluted. For the calculation of the final concentrations the presumed molecular masses are given in Table 7, for the polymer with the unknown molecular mass a presumed molecular mass was set at 15,000 for both. The used volumes of the as-received polymer solutions are shown in Table 8.

Table 8: Volume of NMP/polymer solutions used for preparing 1 mg/mL dilutions in 1 mL THF

Polymer	NMP stock solution [µL]
PVP	12.5
PMMA	6.7
PI	10.0
PS	5.0
PVA	6.7

Polymer powders

Another set of samples were polymer powders. The four polymers except the PVP were used here as well. The powders were ground together with the matrix powder at a weight ratio of 1:10. Then the powder mixture was pressed onto the steel target with the help of another target.

Polymer thin films on Si-wafers

Finally, also pre-prepared polymer thin films on Si-wafers were analysed. The same four polymers (without PVP) were studied. The matrix solutions were used at the same concentration as described for the polymer solutions. For analysis, two to four 0.5 µL drops of the matrix solution were dripped onto the film and dried, with an intermediate drying step after every drop.

Figure 7: (Left) Pristine Si-Wafer without a polymer film and (right) a sample holder used for the Si-wafer to transfer the sample to the ion source of the MALDI-linTOF instrument.

6 Instrument settings

6.1 Polyethylene glycol measurements

The following mass spectrometric settings remained unchanged throughout all the measurements:

Mass range	100-3500
Tuning	linear
Spots	Raster in regular cycle
Shots to accumulate	20
Laser repetition rate (Hz)	100
Blast shots	None
Profile number	50
Blanking mass	100
Software	MALDI Solutions Data Acquisition ICS version 2.8.0.5412

The following settings were varied between the measurements:

Raster	Offset of 0.5 µm for the measurements on the same spot
Pulsed extract	400; 600; 1000; 2,000; 20,000 (depending on the mass)
Laser power	Depending on the matrix

The following laser power settings were used for the given matrix:

DHB	40 and 50 a.u.
SA	40 and 50 a.u.
CHCA	40 and 50 a.u.
IAA	30 and 40 a.u.
HABA	30 and 40 a.u.
Norharman	10 and 20 a.u.
DCTB	10 and 20 a.u.

6.2 High molecular weight polymer measurements

The following mass spectrometric settings remained unchanged throughout all the measurements:

Tuning	linear
Shots to accumulate	20
Laser repetition rate (Hz)	100
Blast shots	5
Profile	50
Pulsed extract	none
Software	MALDI Solutions Data Acquisition ICS version 2.8.0.5412

The following settings were varied between the measurements:

Mass range	Changed depending on the molar mass of the polymer
Spots	Raster in regular cycle or on the spot depending on whether the sample is on a steel target or on a Si-wafer
Laser power	Changed depending on the sample, between 95 a.u. and 100 a.u.
Blanking mass	Depending on the mass range

7 Results and Discussion

7.1 Polyethylene glycol

7.1.1 Matrix measurements

Only the matrix itself was measured by MALDI-linTOF MS. These experiments were carried out to optimise measurement conditions for each matrix and to select a laser power used in the subsequent experiments, based on the signal to noise ratio. Also, the calibration of the instrument was done with the matrix after identifying the matrix peaks, shown in Table 9. Measuring the MALDI matrix on its own, one can determine the background signals, matrix clusters and contaminants, all to be considered as chemical noise in the following polymer measurements. Mass spectra fo all the different matrices are shown in Figure 8.
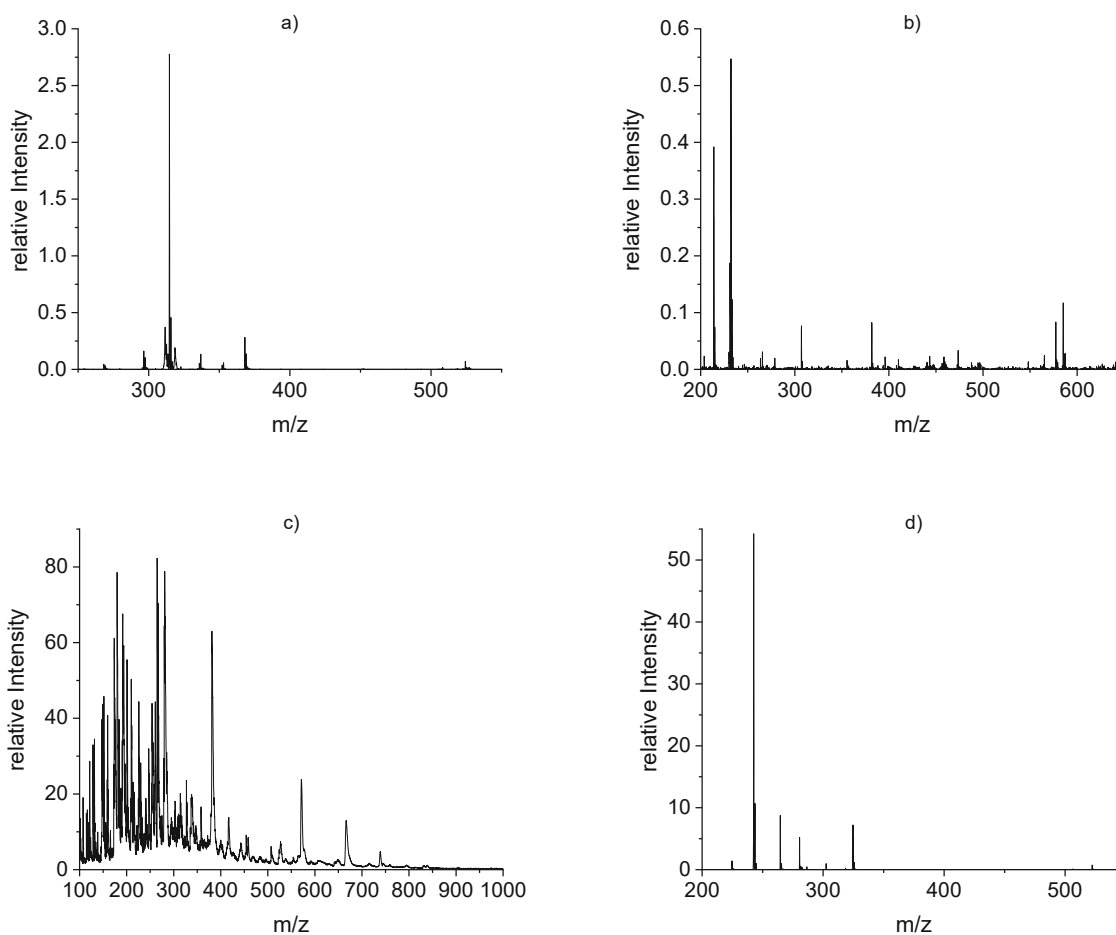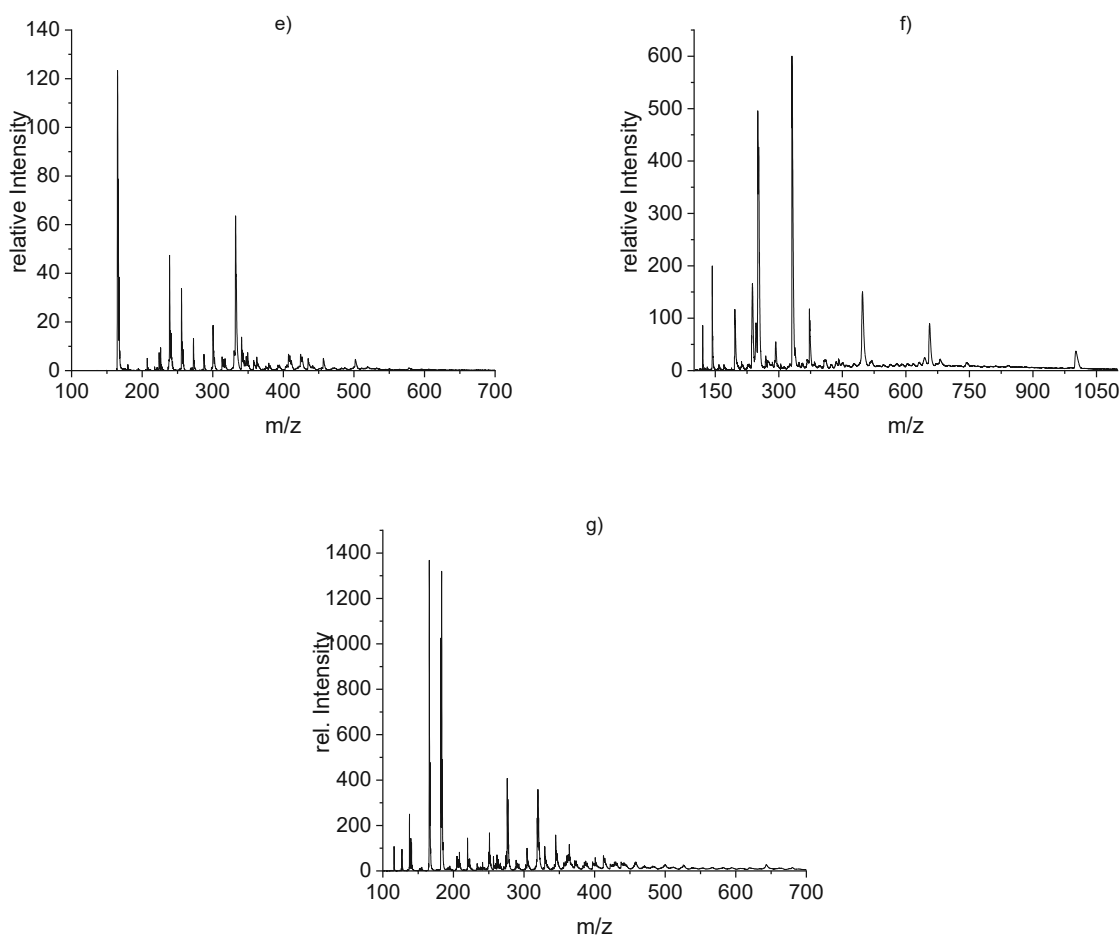
Figure 8: Mass spectra of different matrices measured at 100 Hz with different laser power a) DHB at LP 30, b) SA at LP 30, c) CHCA at LP 30, d) HABA at LP 20, e) Nor at LP 50, f) DCTB at LP 20 and g) IAA at LP 40

Table 9: Identified matrix peaks used for the calibration of the MALDI-linTOF measuerment

Matrix	M	M+2Na+H+	M+2H
DHB	154	200	156
SA	224	271	226
CHCA	189	236	191
HABA	242	289	244
Nor	168	215	170
IAA	175	222	177

For DHB, a high abundant signal for the protonated matrix compound is observed and there are not many fragments, clusters or artefacts visible in the spectrum. SA shows matrix clusters at higher m/z, but the most prominent peaks are observed in the lower mass range. CHCA shows a rich spectrum from very low molecular weight ions up to m/z 800. Most importantly, the baseline of the spectrum is significantly influenced by in-source and post-source decay fragmentation. From this, it can be concluded that it is not ideal to measure low molecular weight samples with this matrix. HABA would be better suited for that,

because of its few, clearly identifiable peaks. Norharman, DCTB and IAA exhibited many signals and are therefore not suitable for samples of lower masses.

7.1.2 Crystallisation of the matrices and polymers

As mentioned in section 4.2.2, the matrix significantly influences MALDI measurements, with crystallization being an important factor. Different matrices result in different sizes and shapes of crystals, thereby impacting the incorporation of the sample. As an example, Figure 9 illustrate that DHB and DCTB yield larger crystals than SA and IAA. This means there is a difference in the embedding of the sample in the crystals, which effects the sensitivity. When the sample and matrix are not well connected through co-crystallization, the transfer of energy to the sample is compromised, leading to reduced desorption/ionization processes. For a better co-crystallization small and uniform crystals are preferred. This is also very important for automated measurements to ensure reliable and reproducible results across multiple samples in a high throughput setting.
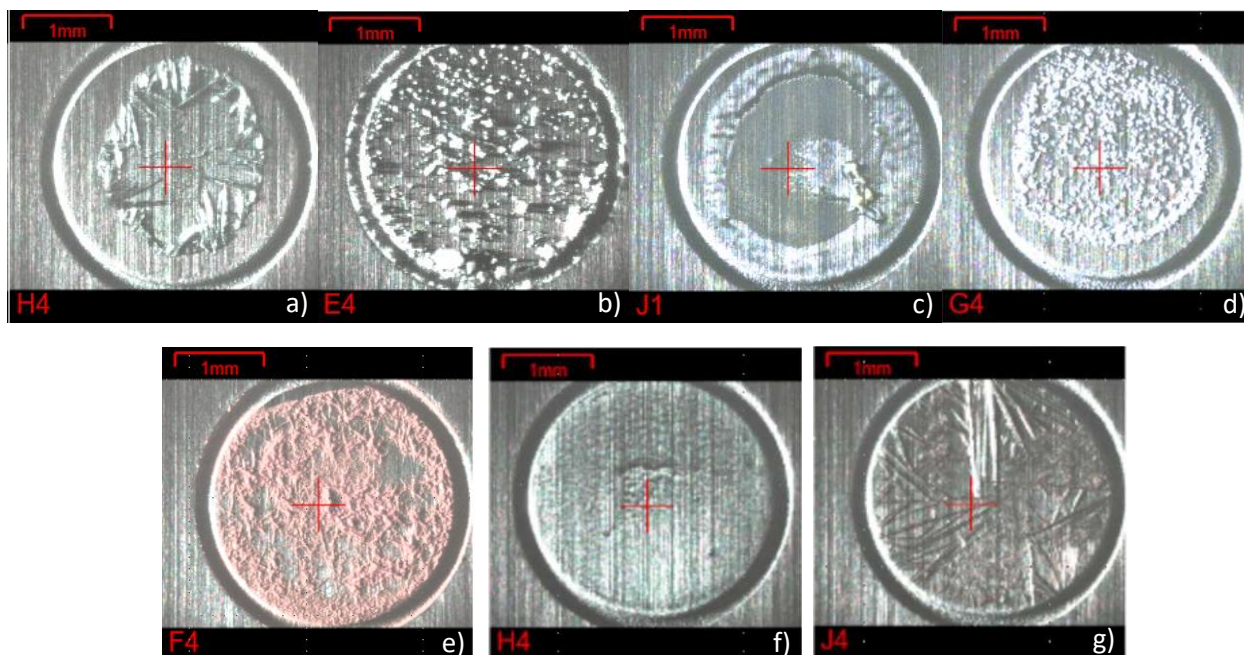
Figure 9: Crystallisation of different matrices a) DHB with EtOH and H_2O, b) SA with EtOH and H_2O, c) CHCA with EtOH and H_2O, d) IAA with THF, e) HABA with THF, f) Nor with THF and g) DCTB with THF

Not only the choice of matrix has an influence on the crystallisation behaviour. Also, the concentration of the matrix has an influence on crystal growth. This is shown in Figure 10 with concentrations of DHB ranging from 5 mg/mL to 20 mg/mL. At lower concentrations the crystals are smaller in size and at higher concentrations DHB forms long spear-form crystals. Adjusting both the concentration and the ratio of the sample with the matrix can help address issues associated with excessively large crystals.
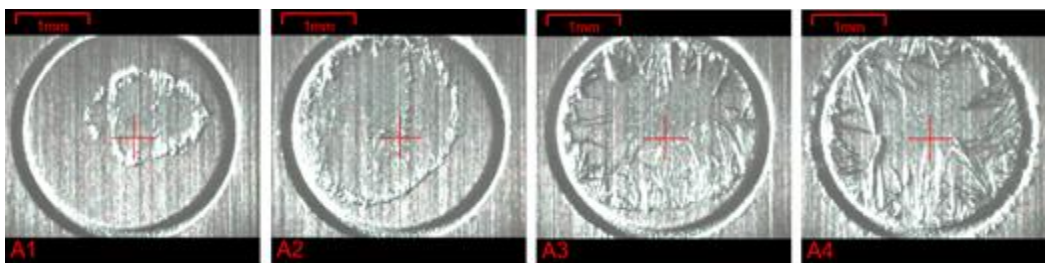
Figure 10: Crystallisation of the DHB matrix A1) only DHB5, A2) DHB5 with PEG, A3) DHB10 with PEG and A4) DHB20 with PEG

The matrix crystallisation is not the sole factor influencing the experiment. The polymer crystals also have a non-negligible influence. This was, however, not done in the work for this thesis, as this would have required extensive extra work and was outside of the scope. But the crystallization of the polymers can impact co-crystallization. Larger crystals may prove advantageous for certain samples. Therefore, when dealing with polymers that exhibit a wide range of mass, sizes and shapes, it is advisable to systematically test various matrices with different concentrations and diverse polymers. This approach allows for a more comprehensive understanding of the interactions between the polymer and matrix, leading to optimized experimental conditions.

7.1.3 Mass spectra

As mentioned, polymers exhibit a mass distribution in the spectra. The highest peak typically corresponds to the molecular mass of the polymer, while the differences between peaks provide information about the monomer mass, which in the case of PEG is Δm/z 44 and can be found in all the spectra Figure 11. All polymer solutions shown in Figure 11 were prepared with a concentration of 1 mg/mL, and the matrix, DHB, had a concentration of 10 mg/mL. The spectra of the measurements with other concentration ratio and matrix can be found in the appendix.

For PEG 400, the most intensive signal is shifted to the left, resulting in a mass lower than m/z 400. Some matrix peaks are also visible around m/z 350. Additionally, there is a secondary mass distribution with lower intensity, shifted by approximately 15-16 mass units from the most prominent peak. This comes from the sodium and potassium adduct ions of the analyte. The monomer mass together with the sodium gives a mass of 67 g/mol and the monomer with the potassium is 83 g/mol. The difference between those masses is exactly 16, which is the shift between the two mass distributions in the mass spectra. The reduced intensity suggests a lower frequency of occurrence of the monomer groups with potassium, compared to sodium, which in comparison is very prominent.

In the case of PEG 600, there is no discernible secondary mass distribution. A single peak appears around m/z 470, which cannot be definitively assigned to a polymer ion. The highest peak is also shifted to a higher m/z. With PEG 1000, the most intense peak is located almost at m/z 1000, accompanied by a distinct secondary distribution with a shift of Δ16 which can be attributed to oxygen. The difference in intensity between the primary mass distribution and the secondary distribution increases with the polymer's mass. PEG 2,000 exhibits an even more pronounced difference, with a visible secondary mass distribution. The low resolving power of the linTOF does not allow to resolve the polymer distribution of PEG 20,000, making it impossible to calculate the monomer mass. And a substantial shift from the original molecular mass to higher m/z is evident.

The different shifts of the molecular mass compared to the measured m/z in the mass spectra can come from variations in the polymer structure and composition. With increasing mass, the overall structure and conformation of the polymer chains may undergo changes, influencing the interaction with the matrix during the MALDI process.
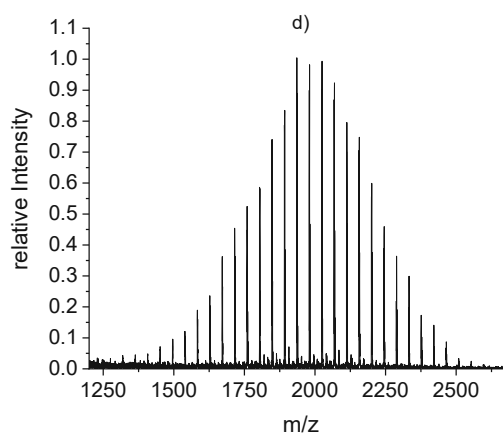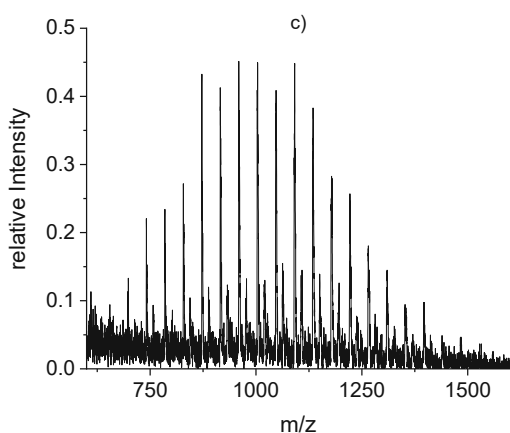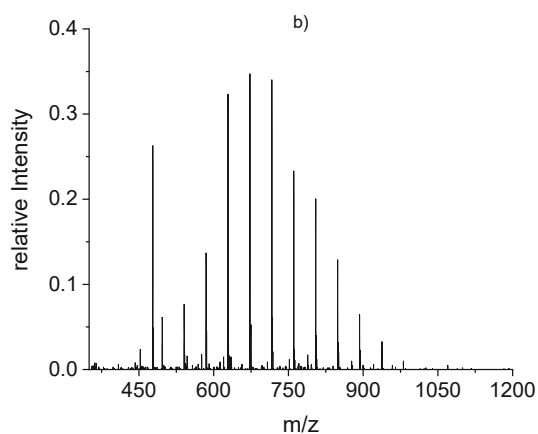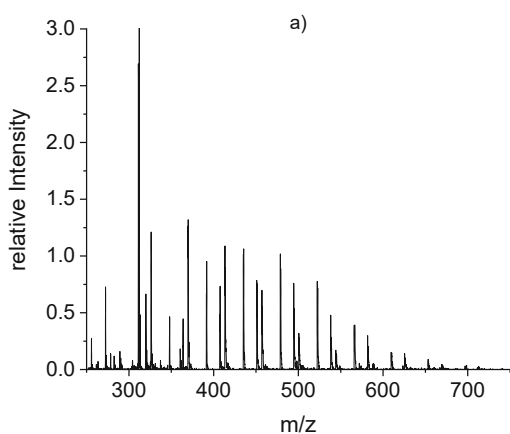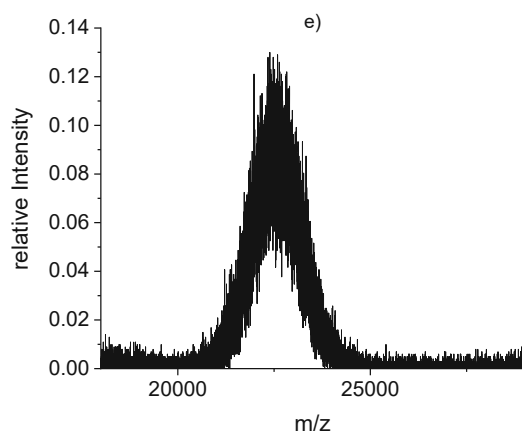
Figure 11: Measurement with DHB 10 mg/mL of different polymer solutions 1 mg/mL a) 400 PEG, b) 600 PEG, c) 1000 PEG, d) 2,000 PEG and e) 20,000 PEG

The predominant mass differences from the spectra observed of PEG 400 with DHB10 are represented in Figure 12.
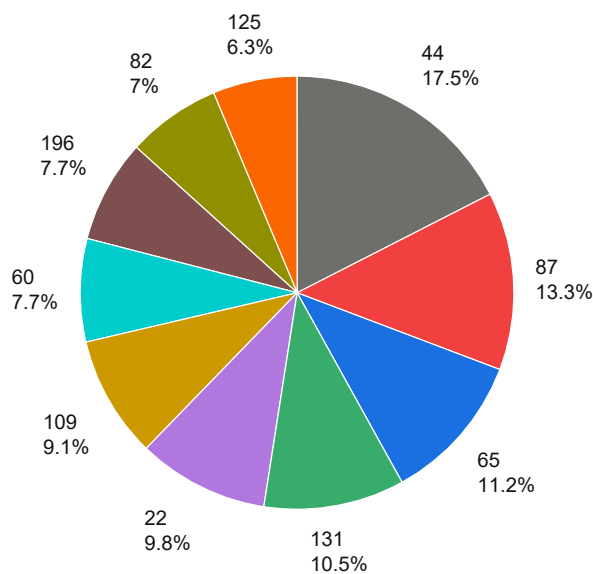
Figure 12: Mass differences observed in mass spectra of PEG 400 measured with DHB (10 mg/mL) with a laser power 40 a.u.; observed Δm/z are shown with the percentage of the sum of all Δm/z occurrences

The most prevalent mass difference is 44, corresponding to the monomer mass. Another common mass difference is 60, representing the oxidized form of the monomer, contributing to the secondary mass distribution. Δm/z of 87 and 131 may indicate the dimers and trimers of the monomer. The presence of sodium giving a Δm/z of 22 allows an interpretation for Δm/z 65 being the monomer with a sodium adduct. Additionally, the peak at m/z 196 is close to the combined mass of the DHB matrix and the polymer monomer.

33

7.1.4 Polymer distribution and maxima

The range of the polymer mass distributions and the most abundant peaks (i.e. the peak maxima) are listed in Table 10 and selected as seen in Figure 13.
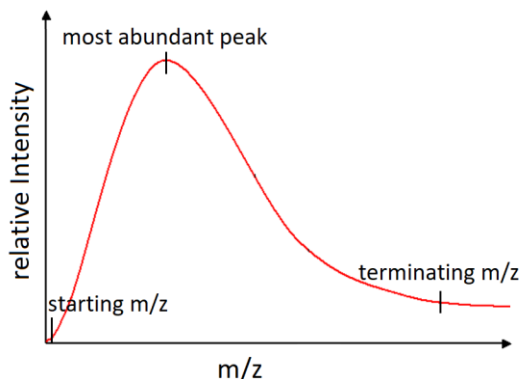
Figure 13: Scheme for determining the polymer mass distribution and the most abundant peak

As an example, the measurements with DHB are discussed. As it can be observed, the most abundant peaks, as well as the starting and terminating m/z values, do not consistently align. They exhibit variability within a range, occasionally featuring outliers, such as m/z 1130 for the measurement of DHB5 and PEG 400D2, which significantly exhibits higher values than the preceding. Moreover, all measurements with dilution 2 consistently present a higher terminating m/z. A similar phenomenon is observed in DHB20 of PEG 2,000, where some abundant peaks deviate from the expected value. Notably, in PEG 600D1 measured with DHB10 and 20.

Table 10: Mass distributions for PEGs measured with different concentrations of DHB

Matrix and Polymer	PEG and DHB concentration	Most abundant peak m/z	Starting m/z	Terminating m/z
DHB 400	ST 5	369.7	304.2	677.5
	ST 10	402.5	293.3	642.7
	ST 20	435.1	304.2	671.0
	D1 5	361.4	295.0	578.7
	D1 10	361.5	273.7	646.5
	D1 20	339.9	275.5	554.6
	D2 5	382.0	302.1	1130.1
	D2 10	428.7	275.2	993.6
	D2 20	382.0	286.9	703.4
DHB 600	ST 5	625.5	451.0	930.7
	ST 10	653.5	435.3	958.7
	ST 20	653.3	435.5	960.2
	D1 5	677.3	380.0	1042.4
	D1 10	956.6	560.1	1128.3
	D1 20	490.3	382.9	555.8
	D2 5	678.0	400.3	1167.8

	D2 10	678.0	399.1	1141.5
	D2 20	678.0	382.4	1011.8
DHB 1000	ST 5	1,047.3	676.0	1,463.0
	ST 10	1,150.7	975.3	1,412.9
	ST 20	1,063.1	833.6	1,326.6
	D1 5	1,064.8	767.2	1,429.2
	D1 10	1,044.3	785.2	1,258.7
	D1 20	978.7	761.7	1,301.7
	D2 5	1,089.6	703.9	1,741.2
	D2 10	1,089.6	703.9	1,662.9
	D2 20	1,142.0	677.9	1,717.0
DHB 2,000	ST 5	2,315.5	1,703.4	2,489.3
	ST 10	2,096.9	1,572.0	2,490.8
	ST 20	1,969.0	1,664.1	2,581.6
	D1 5	2,097.1	1,583.1	2,484.2
	D1 10	1,968.5	1,624.2	2,312.6
	D1 20	1,947.0	1,474.4	2,420.7
	D2 5	2,215.6	1,507.5	3,114.7
	D2 10	2,294.4	1,507.0	3,166.9
	D2 20	2,294.8	1,637.9	3,007.7

For easier comprehension, some examples featuring different matrices and polymer masses are visualised in the following figure. Using CHCA as matrix is more effective for polymers with higher molecular masses, as previously indicated. Yet, there is an excessive cut-off at the lower m/z of the mass distribution because there is no differentiation between matrix peak and polymer peaks. And the polymer distribution is not symmetric (Figure 14a) for all the measurements. In contrast, the distribution of PEG 2,000 are symmetric (Figure 14b). For SA, the broadness of the mass distribution changes from the stock solution to dilution 1 and 2 (Figure 14c). For the dilutions the most abundant peak is shifting to higher masses, by approximated ∆m/z 250 compared to the stock solution. This discrepancy suggests that the polymer/matrix ratio plays a crucial role for determining the maximum and broadness of the polymer distribution. For dilution 1 with PEG 600 and concentrations of DHB at 10 and 20 mg/mL the mass distribution shows an inconsistency in the broadness and the position of the most abundant peak (Figure 14d). This may be indicative of a measurement error. Most importantly, it is also observed that measurements with CHCA have the most constant determination of the maximum of the distribution being rather independent from polymer and matrix concentration (Figure 14 a and b compared to c and d), yet not being at the same maximum as with other matrices (Figure 14 b and c).
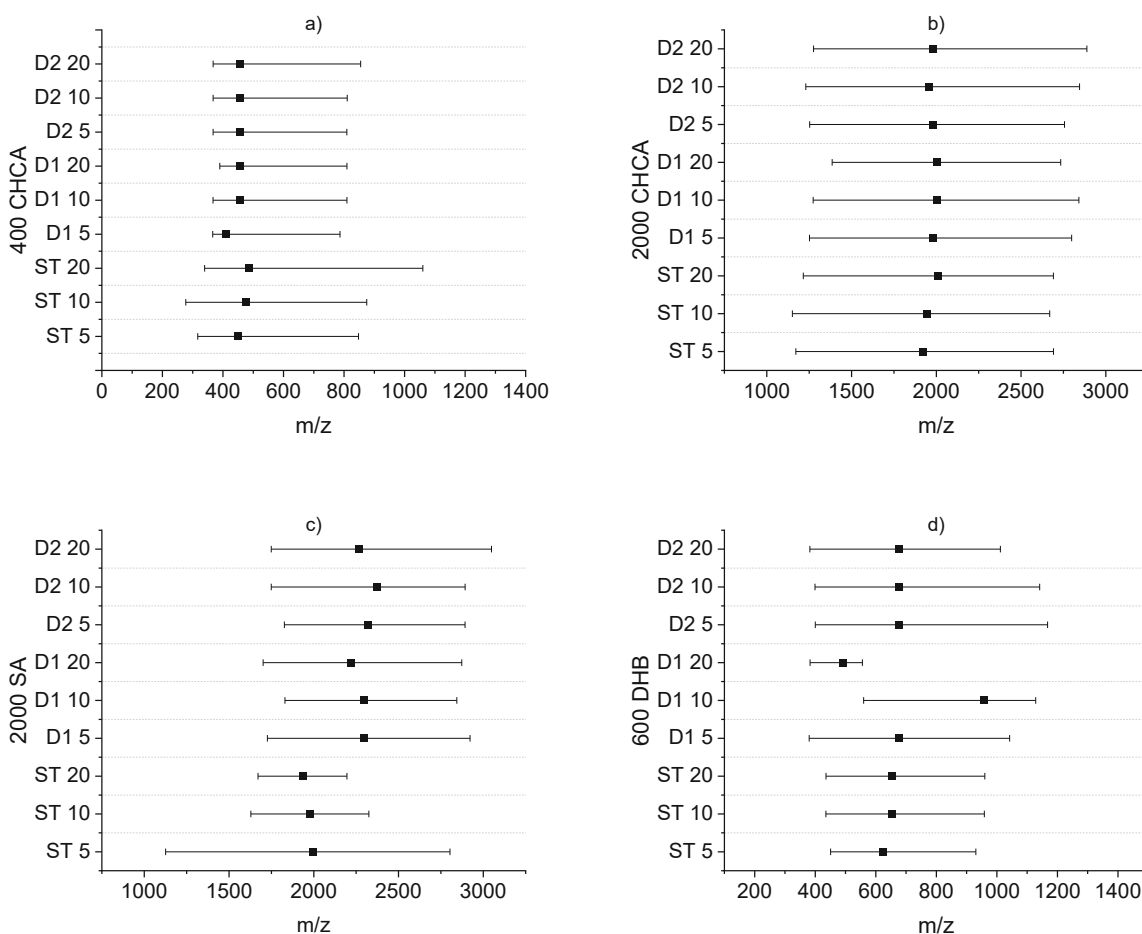
Figure 14: Mass distributions (width of bar) and maxima (black square) of a) PEG 400 with CHCA, b) PEG 2,000 with CHCA, c) PEG 2,000 with SA and d) PEG 600 with DHB

7.1.5 Calculation and comparison of M_n and M_w

Molecular weight parameters, namely M_n, M_w, and PD, were calculated and compared. Despite the expectation that these matrices would remain unaffected by variations in concentration and the matrix-to-sample ratio, discrepancies were observed. In all measurements, M_w consistently appeared at a higher m/z than M_n. Notably, the PEG 2,000 with DCTB matrix displayed a relatively consistent measurement of M-values, although uniformly lower than the nominal molecular mass of the polymer provided from the supplier (Figure 15a). The Norharman matrix yielded M-values that formed three distinct clusters across all polymer solutions. The stock solution of PEG 2,000 exhibited the lowest M_n and M_w values, with the 5 mg/mL matrix concentration consistently contributing to the lower m/z within each cluster. Furthermore,

36

the stock solution cluster exhibited a more pronounced deviation from the other polymer solutions compared to dilutions 1 and 2, still with similar trends within all three respective clusters.
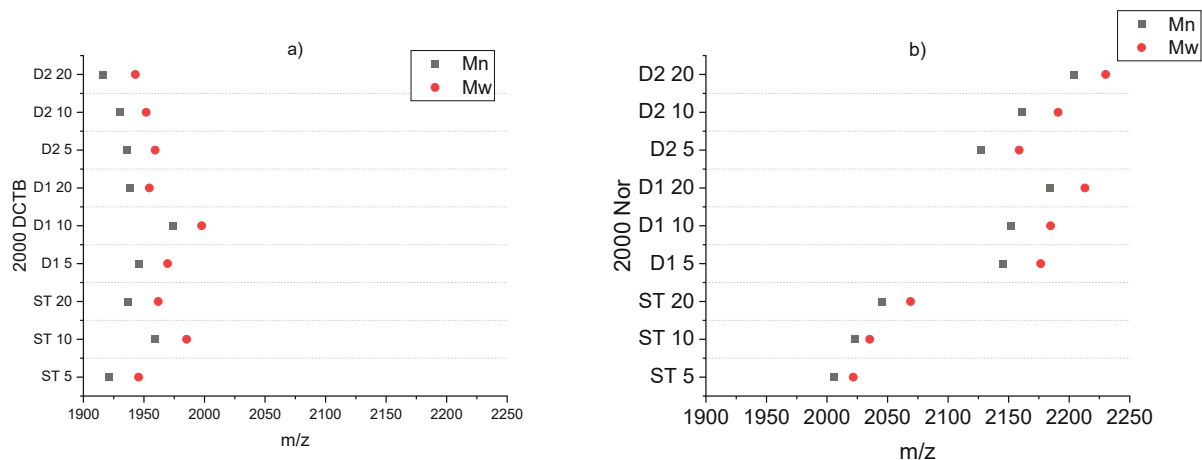
Figure 15: M_n and M_w for PEG 2,000 (ST, D1, D2)) measured with different concentrations (5 mg/mL, 10 mg/mL and 20 mg/mL) of a) DCTB and b) Nor

These variations, cluster formations, and trends may stem from factors such as solvent effects, polydispersity, calibration issues, ionization efficiency, instrumental settings and sample purity. Each of these could be further investigated. However, the primary objective of this work is to highlight the influence of different matrices and their concentrations on a polymer solution with varying concentrations. Consequently, for each polymer the focus lay on identifying the optimal matrix for the specific polymer and subsequently determining the appropriate ratio between the matrix and the sample. Further experimental data are shown in the appendix.

The polydispersity index (PD) is expected to be close to 1, indicating the uniformity of a polymer. This measure should ideally remain constant regardless of changes in concentration or molecular weight. In this context, CHCA exhibits more promising results than DHB (Figure 16). DHB displays an outlier at ST 20 for PEG 1000 and broader distributions for D2 5 and 10. Such outliers can be explained by the fact that the number of repetitions was too low to eliminate or reduce a large deviation. Further results for PD-values are displayed in the appendix.

37
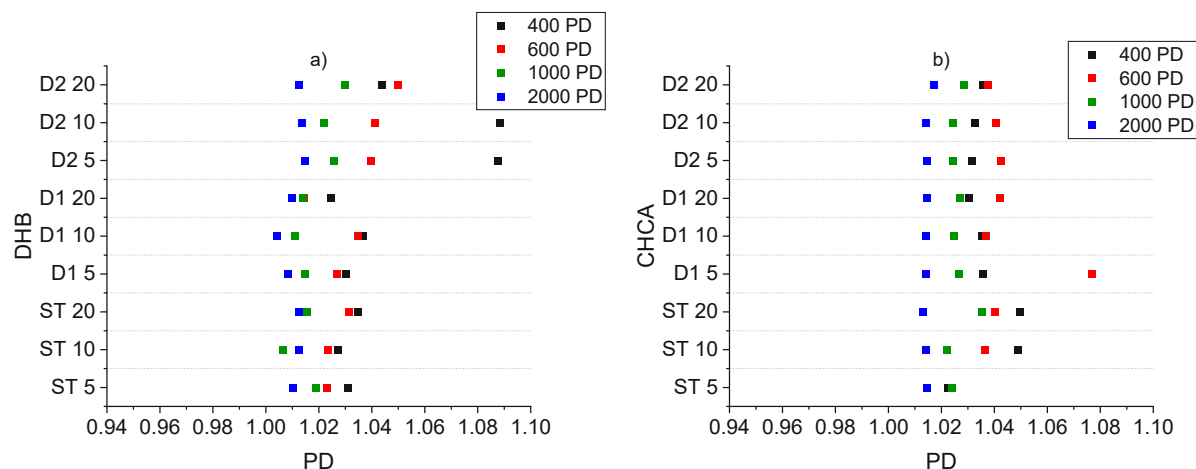
Figure 16: PD values determined for PEG (ST, D1, D2) with varying concentrations (5 mg/mL, 10 mg/mL and 20 mg/mL) of a) DHB and b) CHCA

7.2 High molecular weight polymers

7.2.1 Measurements with polymer solution and polymer powder

High molecular weight polymers were provided as NMP solutions. To determine the chemical noise coming from the solvent, the first step was to measure pure NMP, without any polymers. Already there the first challenge was encountered: NMP is not volatile. This means, that it takes energy from a heating plate or two days of waiting time for it to dry. Only then it was possible to measure NMP by MALDI linTOF MS. The same difficulties were observed for the polymer solutions. Even after extensive drying periods no mass spectra were obtained for the polymers. This approach was therefore not further pursued.

Sample preparation method was changed to the powder approach. Spectra of PMMA and PI were successfully obtained, as shown in Figure 17.
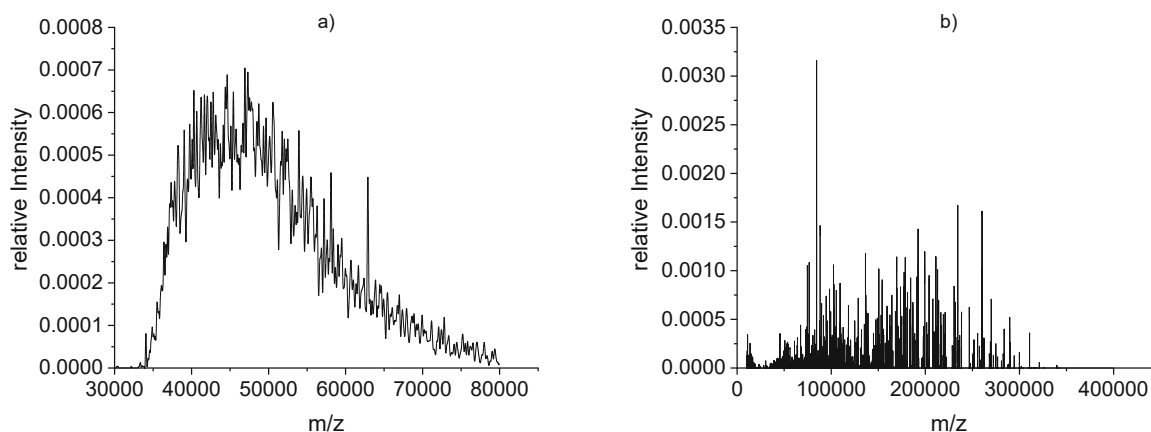
Figure 17: a) PMMA with IAA (1:10) at LP 75 and b) PI with DHB 10 mg/mL at LP 95

The PMMA spectrum exhibits an expected mass distribution, with the maximum indicative of the molecular mass of the polymer at approximately m/z 45,000. However, the detected maximum is slightly higher than expected. The molecular weight was expected to be approx. m/z 10,000—35,000. The overall form, though, aligns with expectations at high molecular weight polymers. On the other hand, PI demonstrates a distribution without a typical polymer distribution, making it challenging to identify the maximum amid some artefacts. Despite this, the spectrum suggests that the molecular mass should be in the range of m/z 100,000 to 200,000. At this molecular weight the measurement of apolar polymers is challenging for linTOF instruments very often not allowing sensitive measurements. Due to the uncertainty of the molecular mass, further statements are not possible.

7.2.2 Measurements with polymer on Si-Wafer

The idea behind these experiments was to measure already applied polymer films directly on Si-Wafer pieces, as described in Chapter 5.3.

The first measurements were performed with thin films made from PEG 2,000 and 20,000 using 10 mg DHB/mL. Compared to the results shown in Chapter 7.1.4, the PEG polymer distributions exhibited mass shifts to lower molecular weights (Figure 18). A plausible explanation for this observation is, that the polymer undergoes heating during the film preparation process. With temperatures of up to 120°C it is possible that the polymer is degrading during this step. To test this, specifically for PEG, an alternative heating approach at 70°C was attempted. For PEG 2,000, a shift to lower m/z, to around m/z 350, was observed at 120°C. At 70°C, two distinct mass distributions emerged at approximately m/z 1250 and 1750 (Figure 18 a, b). In the case of PEG 20,000, the mass distribution shifted to m/z 400 for the polymer prepared at 120°C, and a lot of signals around m/z 140 appeared for the preparation at 70°C. While impurities are also a possibility, it is more likely that the heat induced changes and degradation in the polymer, because they do not match the signals from the matrix without polymer film. The instability of PEG 20,000 could explain the mass distribution at 70°C, but not the lesser ions at 120°C. One hypothesis is that, at the higher temperature, the polymer recombines into smaller, more stable chains, whereas at 70°C, it simply breaks up into smaller ions. Another possibility is that the signals at the lower m/z of 20,000 cured at 70°C are from the matrix and there is no possibility to measure this polymer cured at this temperature. This is very possible, because some of the peaks match the matrix signals.
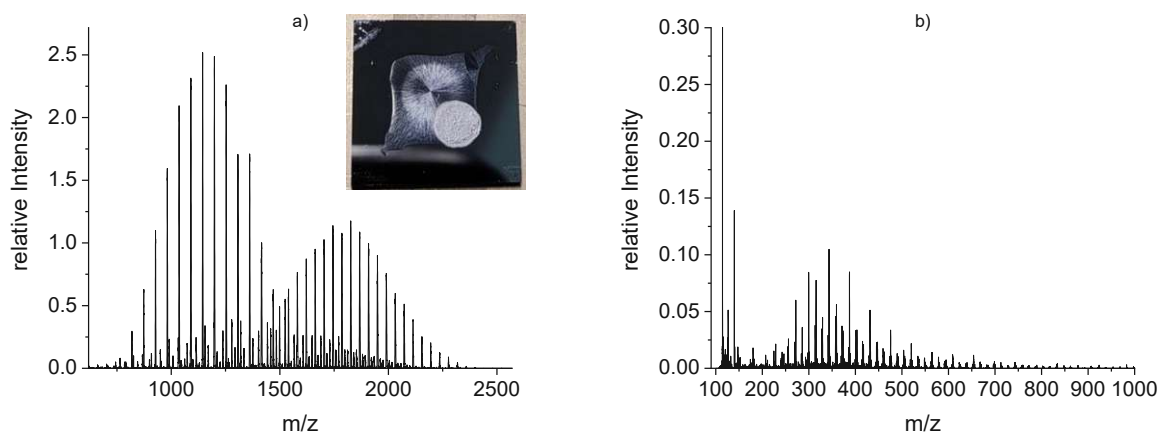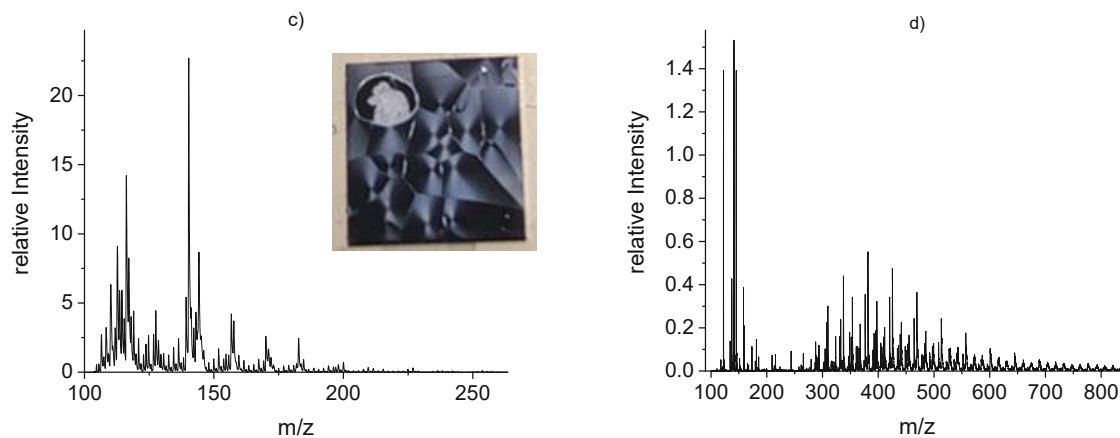
Figure 18: Si-Wafer thin films of PEG measured with DHB 10 mg/mL a) 2,000 cured at 70°C measured with LP 80, b) 2,000 cured at 120°C measured with LP 85, c) 20,000 cured at 70°C measured with LP 95 and d) 20,000 cured at 120°C measured with LP 95

The next measurements involved the high molecular weight polymer films applied on the Si-Wafer. For the PI film, in contrast to the powder measurement, there is now an expected mass distribution, with the maximum around m/z 100,000. This expectation for the molecular mass was already confirmed during the measurements using matrix powder. However, measuring PI film on a Si-Wafer proved possible only with the DHB matrix (as the powder measurement) and not with the other matrices. The PI mass spectrum is shown in Figure 19. The mass spectrum was smoothed using a Savitzky-Golay filter with a mass increment of 150 and in 5 cycles resulting I a rather broad polymer distribution with no distinct mass differences for the monomer unit. No measurements were successful for PMMA. For PS some low molecular mass ions were discernible with DCTB as matrix, but no mass distribution in the expected mass range of 800-5000 was recorded. The sample P1 was also measured with different matrices, out of which only DHB allowed successful measurements. After using the same smoothing parameters, a mass distribution with a maximum at m/z 100,000, similar to the one observed for PI, was detected.
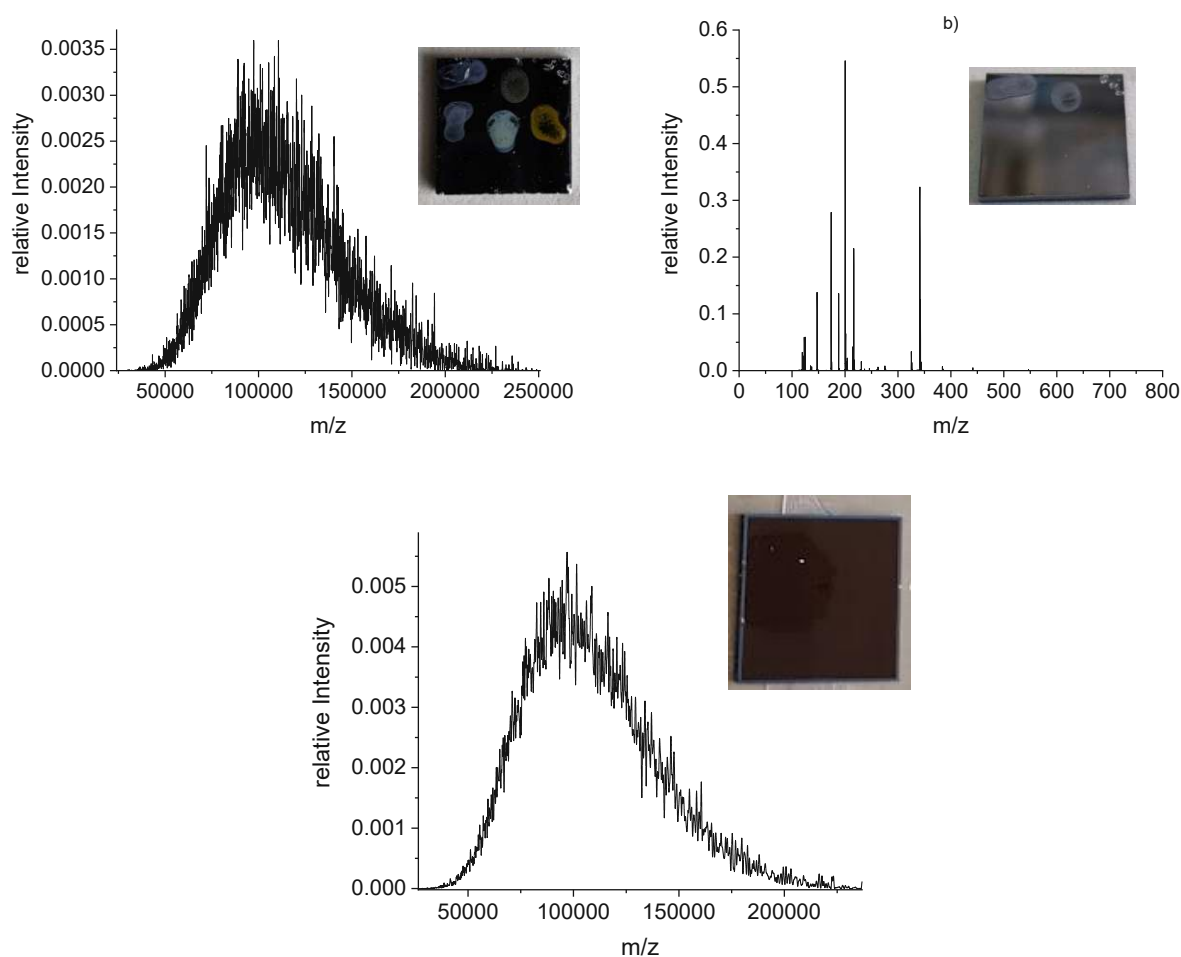
Figure 19: Si-Wafers with polymer films and different matrices: a) PI thin film with DHB 10 mg/mL measured with LP 100 (Savitzky-Golay smoothing) b) PS with DCTB 10 mg/mL measured with LP 95 and c) P1 with DHB 10 mg/mL measured with LP 100 (Savitzky-Golay smoothing)

7.2.3 Ageing of polymer films

7.2.3.1 7 days UV-light exposure

PI, PS, and P1 polymer films cured at 70°C and 120°C, together with PEG 2,000 and PEG 20,000 were exposed to UV light for one week. Figure 20 shows that in the case of the PEG 2,000 two mass distributions were observed with a maximum at m/z 1750 for the samples cured at 70 °C. These results are comparable to results for untreated PEG 2,000. Although oxidation effects were expected, no discernible change to the polymer distribution was induced by the one-week exposure to UV light. However, for PEG 2,000 cured at 120°C, no polymer distribution was observed for the samples treated with UV light. Only some signals remained at m/z < 250, indicating a change compared to the untreated PEG. Since signals at similar m/z were observed already in the untreated PEG 2,000 it is concluded that the UV-light furthered the effect that occurred during the high temperature curing.
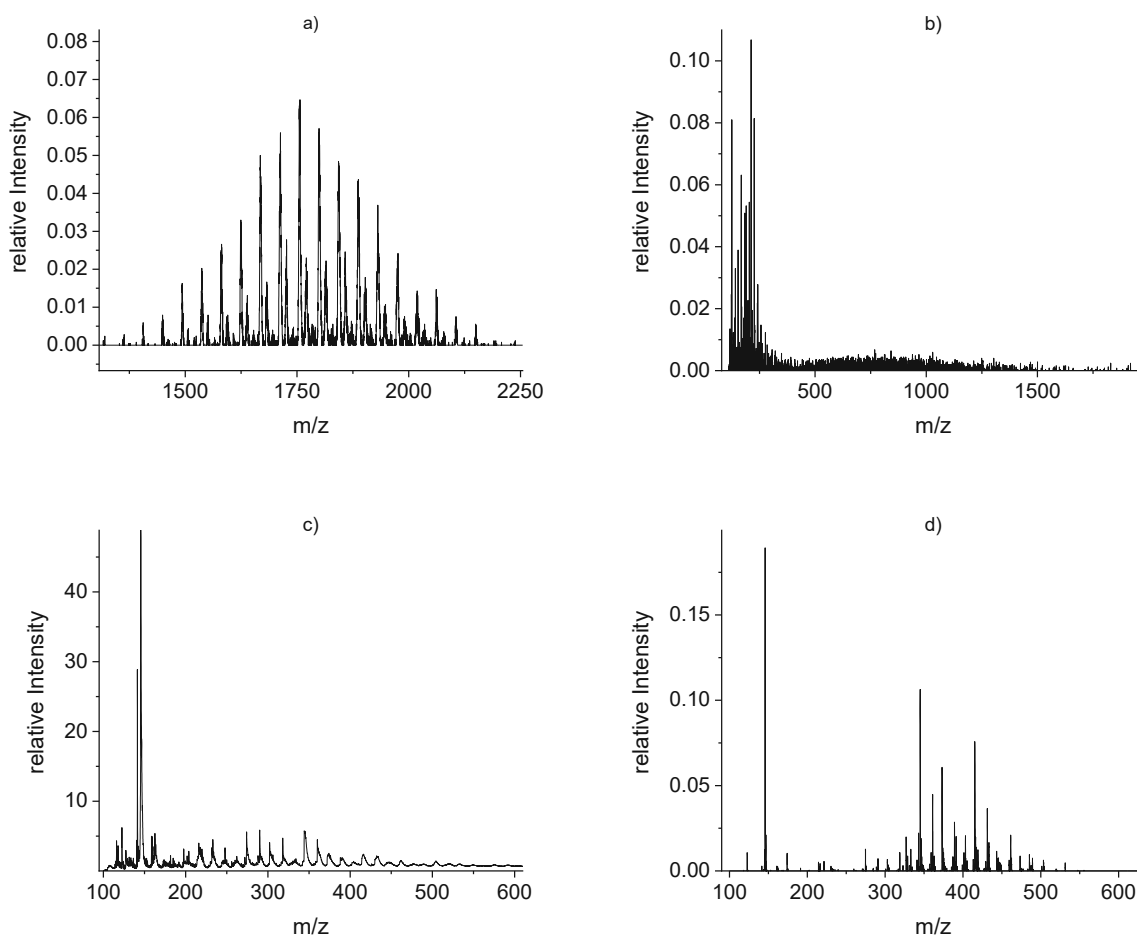
Figure 20: Si-wafer prepared with PEG films measured with DHB 10 mg/mL after 1 week of UV light exposure a) 2,000 cured at 70°C measured with LP 80, b) 2,000 cured at 120°C measured with LP 85, c) 20,000 cured at 70°C measured with LP 95 and d) 20,000 cured at 120°C measured with LP 95

The PEG 20,000 film cured at 70°C still exhibits signals at lower m/z, along with additional ones observed around m/z 300 (Figure 20). The PEG 20,000 film cured at 120°C maintained a mass spectrum showing its typical distribution with a monomer mass of 44. However, the distribution gets smaller and less mass differences are observable. These observations suggest that the polymer undergoes some smaller changes, but still remains stable after exposure to UV-light.

PI exhibits a slight shift to higher m/z, with the centre of the mass distribution not at 100,000 but slightly higher at around m/z 112,500 (Figure 21). This is still within the measurement accuracy for the maximum. Aside from this shift there is no significant change observed after exposure to UV light for a week.
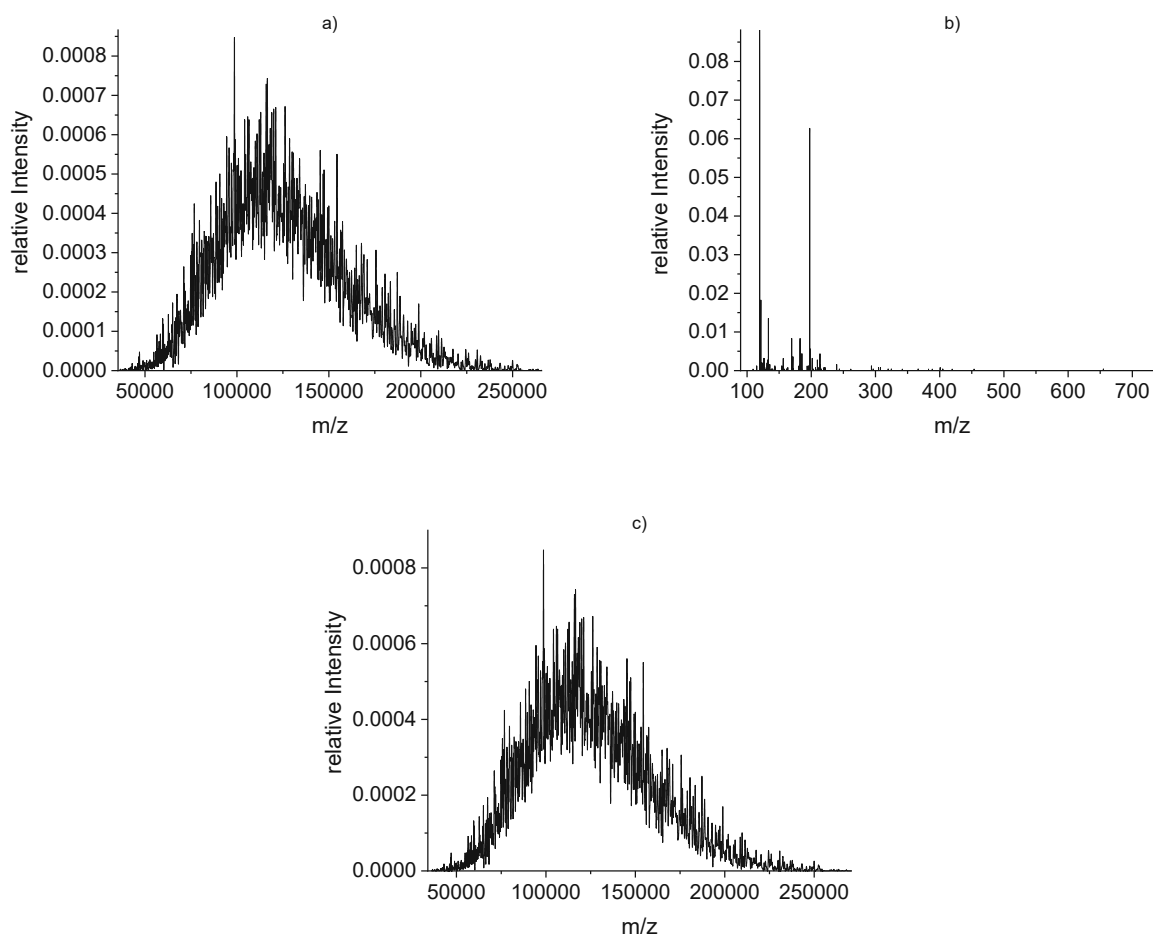
Figure 21: Polymer films measure after one week of UV exposure a) PI measured with DHB 10 mg/mL and LP 100 (Savitzky Golay smoothing), b) PS measured with DCTB 10 mg/mL and LP 95 and c) P1 measured with DHB 10 mg/mL and LP 100 (Savitzky Golay smoothing)

The m/z values measured for PS shifted to smaller values, with more signals appearing at m/z ≤ 200. Signals around m/z 345 were no longer observed. It was concluded that changes occurs after UV exposure. P1 remains unchanged after exposure to UV light except a slight shift to m/z 125,000, again within the measurement accuracy for the maximum. This implies that no change has occurred.

7.2.3.2 14 days UV-light exposure

After exposure to UV light for two weeks, the PEG 2,000 on the Si-Wafer exhibited obvious changes visible by eye. These changes were not reflected in the mass spectra, at least not for the polymer film cured at 70°C. It retained the mass distribution at m/z 1750, along with the secondary mass distribution. In the case of the PEG 2,000 film cured at 120°C, the mass distribution shift to lower m/z is still observable, but mass resolution is not sufficient enough to identify the monomer mass. On the other hand, PEG 20,000 films undergo significant changes after UV exposure. There is one prominent peak around m/z 500 for both curing temperatures, accompanied by some matrix cluster and fragments at lower m/z, but most significantly, the polymer distribution does not allow to decipher monomers and has a broad distribution towards higher m/z alues (tailing). Therefore, we can conclude that both a visible change on the Si-Wafer

occurs and a change in the mass spectra is observed. This indicates that PEG 20,000 films are not stable under these conditions.
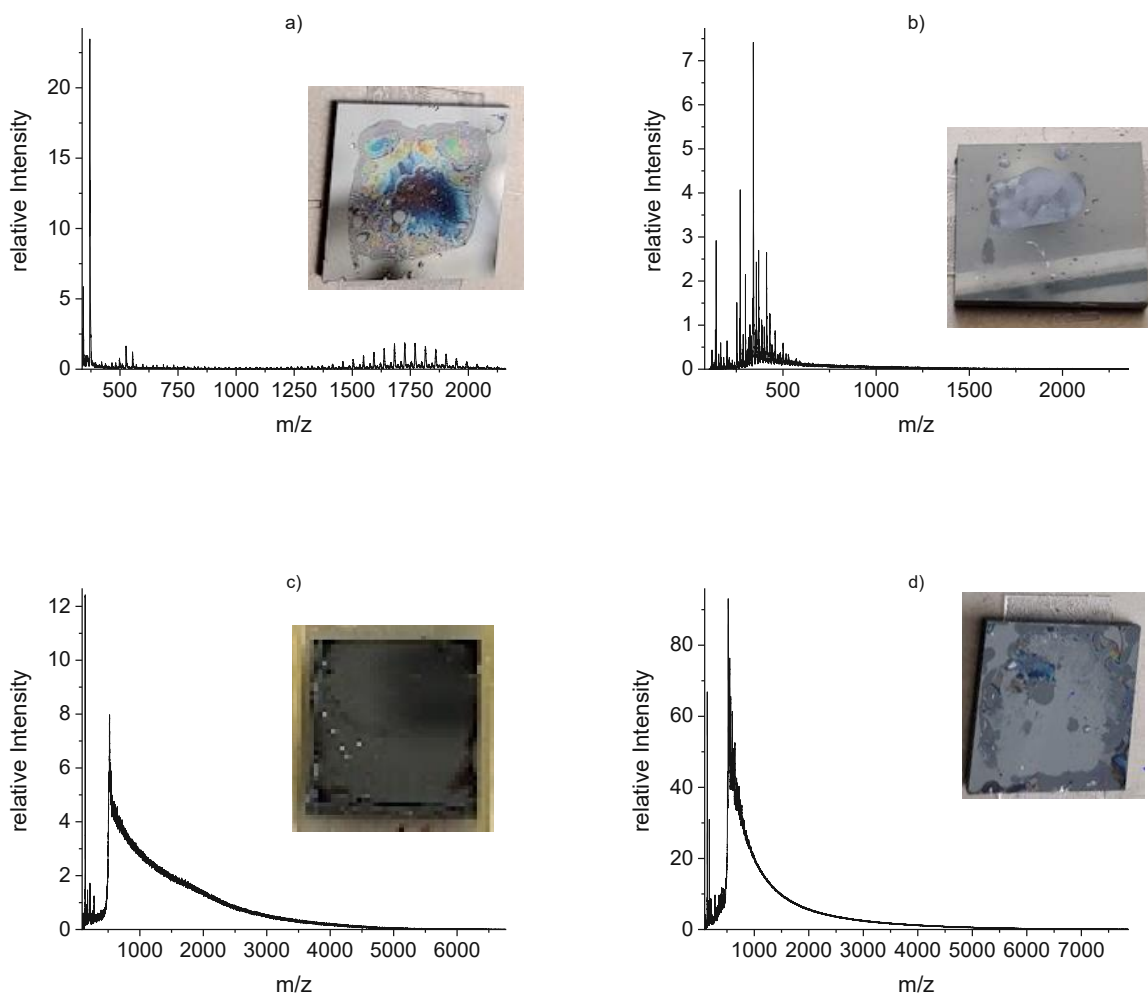
Figure 22: PEG thin films measured with DHB 10 mg/mL after 2 weeks of UV light exposure; a) PEG 2,000 cured at 70°C measured with LP 80, b) PEG 2,000 cured at 120°C measured with LP 85, c) PEH 20,000 cured at 70°C measured with LP 95 and d) PEG 20,000 cured at 120°C measured with LP 95

PS thin films show even more signals after UV exposure and again monomer mass units cannot be identified. It has to be mentioned that these signals can also result from the matrix alone or the polymer/matrix mixture. The mass distribution of PI is unchanged after UV exposure, but exhibits more signals than before that can be considered as spikes, even after smoothing with Savitzky-Golay. However, there is a noticeable alteration in the colour of the film from mostly transparent to yellow. The P1 mass distribution is also less smooth than before, even after smoothing. There were no other changes observed on the Si-Wafer or in the mass distribution.
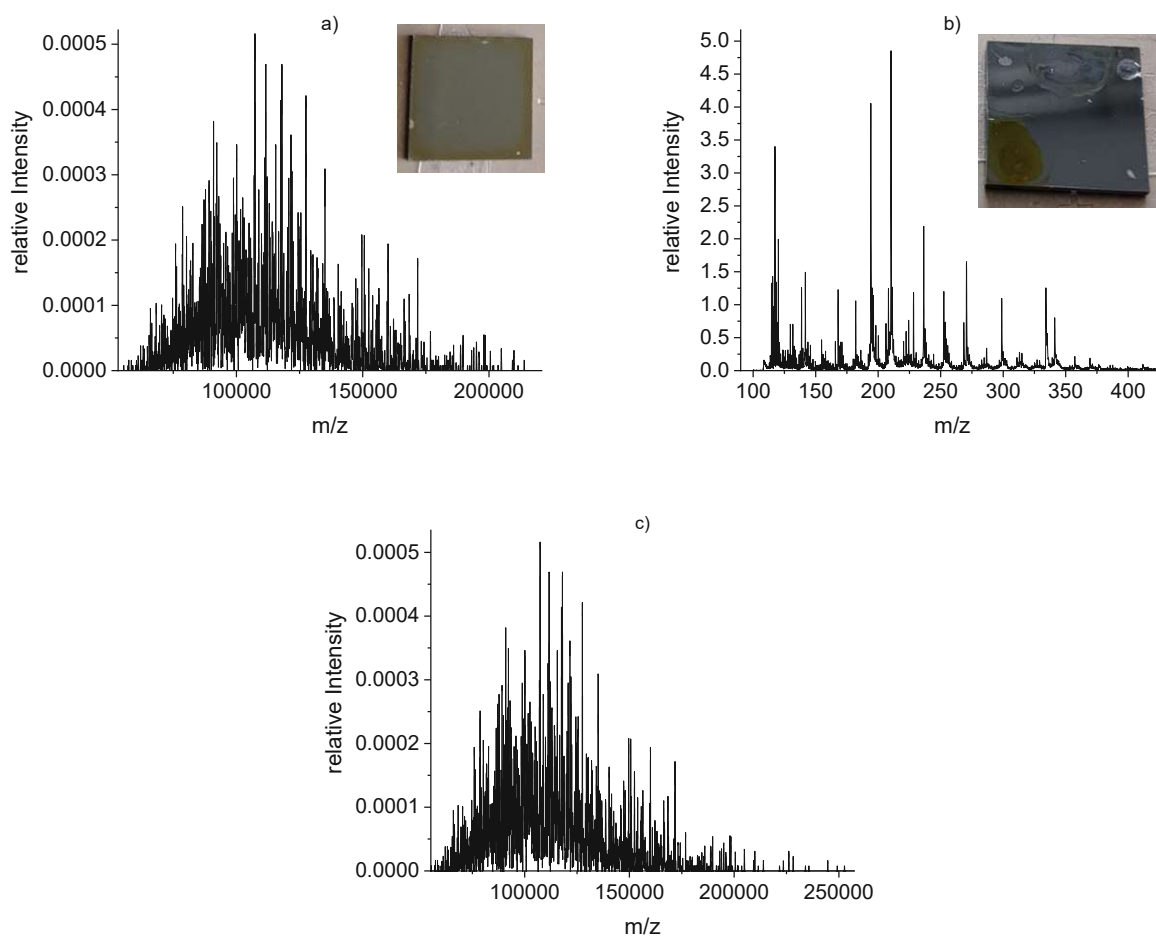
Figure 23:Polymer films to UV-light for two weeks a) PI film measured with DHB 10 mg/mL at LP 100 (Savitzky-Golay smoothing), b) PS film measured with DCTB 10 mg/mL at LP 95 and c) P1 film measured with DHB 10 mg/mL at LP 100 (Savitzky-Golay smoothing)

7.2.3.3 Exposure with 85% SO_2 for 48h at 85°C

The samples were exposed to an 85% SO_2 gas atmosphere for 48 hours at 85°C. PI and P1 showed no changes after this treatment. The mass spectra show a lower number of spikes compared to those after exposure to UV light and are very similar to the native film measurements on the Si-Wafer. This indicates that both polymer films are stable against SO_2 exposure.
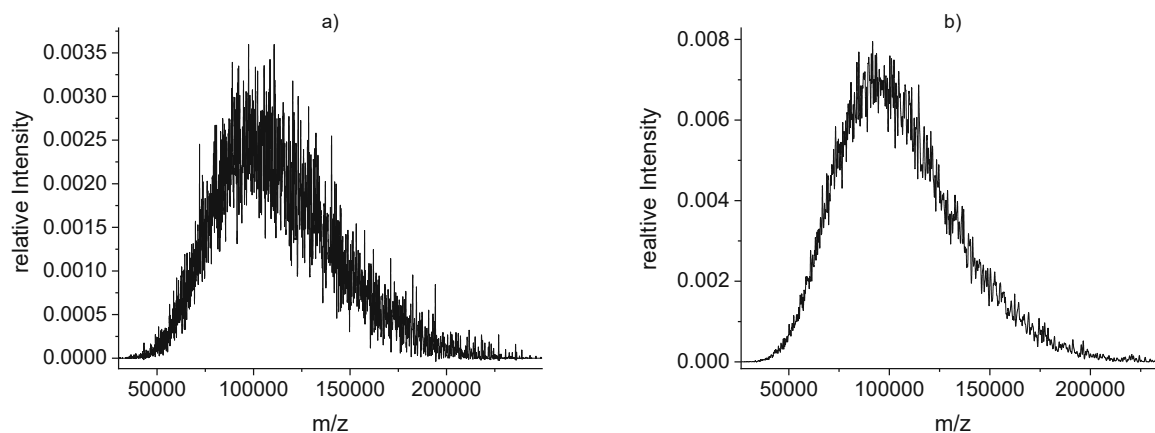
Figure 24: Polymer films prepared with DHB 10 mg/mL after 48 hours of 85 % SO$_2$ exposure at 85 °C measured with LP 100 of a) PI and b) P1

7.2.3.4 Exposure with 85% H$_2$S for 48h at 85°C

The samples were exposed to an 85% H$_2$S gas atmosphere for 48 hours at 85°C. PI and P1 showed no changes after this treatment. The only alteration occurred in the smoothness of the mass distribution. This indicates that both polymer films are stable against H$_2$S exposure.
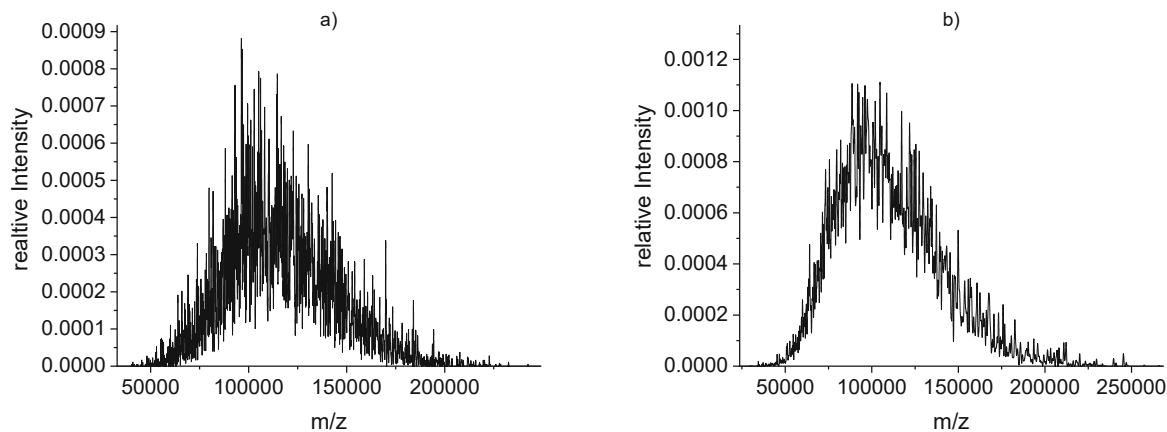
Figure 25: Polymer films prepared with DHB 10 mg/mL after 48 hours of 85 % H$_2$S exposure at 85 °C measured with LP 100 of a) PI and b) P1

8 Conclusion and outlook

In the context of this thesis, low and high molecular weight polymers were investigated using MALDI-linTOF MS. The effect of different matrices and matrix concentrations on the mass spectra was studied for low molecular weight polymers. For high molecular weight polymers, the suitability of different preparation methods for MALDI MS experiments were tested and the effect of UV, H_2S and SO_2 on the polymer stability was investigated.

The use of DHB, SA, CHCA, IAA, HABA, Norharman, DCTB as matrices was successful for measurements of PEG, except for Harmaline. Matrix measurements without polymer were used to optimise the laser settings and the detected ions were used as an internal standard for all measurements. Since crystal size and form are important for the sensitivity and reproducibility of MALDI measurements, the crystallisation of the matrix was carefully studied. DHB and DCTB form bigger crystals than IAA and HABA, which are thus preferred matrices. Further measurements showed that concentration changes or different solvents can be used to tune the crystal size. Polymer concentrations were also influencing the matrix crystallisation, but this effect was not looked at any further.

PEGs with molecular masses from 400 to 2,000 g/mol, showed characteristic mass distributions with a $\Delta m/z$ of 44, the mass unit of the PEG monomer. Only the PEG 20,000 did not show a distinct peak distribution due to the low resolving power of the applied mass analyzer, but still, the mass distribution was at m/z 20,000 or higher depending on the applied matrix. The experiments showed that some matrices, such as CHCA, are clearly better suited for high mass polymers. Additionally, differences for measurements with different matrix and polymer concentration were observed. Matrices and matrix/polymer concentration ratios were investigated for M_n and M_w determination. In some cases, there are trends observable, like the clustering of the polymer concentrations. So that the same polymer solutions have a similar Mn and Mw, like for Nor and PEG 2,000 g/mol. But for DCTB for example no clustering occurs and the Mn and Mw are similar independent of the polymer or matrix concentration. From the M_n and M_w, the PD of the PEG was calculated, which gives information about the uniformity of the polymer. Our results showed, that all the PEG samples were homogeneous.

The measurements with the high molecular weight polymers was challenging. Especially the increasing apolar character of the polymers is hindering efficient desorption/ionization. The polymers of interest are only scarcely described making sample preparation difficult. The first experimental series was performed with polymer solutions in NMP which was not successful. Pressing a powder mixture of matrix and polymer on a target was more successful. By this PI and PMMA could be measured. Lastly, thin films of the polymers on Si-wafer as carrier were measured. Thin film measurements of PEG 2,000 and 20,000 were used to compare the measurements of the films with the measurements of the polymer solutions. It was found that the PEG distribution was not directly comparable to the distribution of the polymer in solutions. Changes occur due to the heating during film curation. This was particularly observed as changes for the maximum of the polymer distribution but also for the width of the distribution. For three industrially relevant polymers, PI, PS and P1, mass spectra were obtained from the respective polymer films. PI and P1 showed a distinct mass distribution.

All thin film samples were UV aged for one and two weeks, and SO_2 and H_2S aged for 48 hours. UV aging showed some changes for PEG already after one week, which were even more pronounced after the

second week. For PS there were some minor changes observable after the first week and after the second week it changed completely. PI and P1 had no changes other than in the level of the background noise and a very small shift, which can also be attributed to the method inherent measurement error. Ageing with SO_2 and H_2S was done only for PI and P1. No changes were observed.

Overall, our results show that measurements of low molecular polymers are possible with MALDI-linTOF MS and give information about the monomer mass and the molecular weight. Depending on the matrix, the measurements need different settings and more or less careful adjustment of matrix and polymer concentrations.

It was shown, that, in general, MALDI-linTOF MS is able to measure high molecular mass polymers. However, the low resolving power of the linTOF does not allow to determine the mass of the monomer units. This gives information on the stability of the polymers, but no information about the structure. Measurements of high molecular mass polymers are not trivial and need optimisations to be possible at all.

Based on the findings in this thesis, additional experiments can be considered to retrieve more comprehensive insights on the investigated topics, especially for the high molecular mass polymers.

9 References

1. Young, R.J. and P.A. Lovell, *Introduction to Polymers, Third Edition*. 2011: Taylor & Francis.
2. Braun, D., et al., *Polymer Synthesis: Theory and Practice: Fundamentals, Methods, Experiments.* Polymer Synthesis: Theory and Practice, 2001.
3. Hillenkamp, F. and J. Peter-Katalinic, *MALDI MS: A Practical Guide to Instrumentation, Methods and Applications*. Second edition. ed. 2013, Newark: Newark: Wiley. 477.
4. Li, L.Q.L., *MALDI mass spectrometry for synthetic polymer analysis*. Chemical Analysis: A Series of Monographs on Analytical Chemistry and Its Applications. 2009, Hoboken: Hoboken : : Wiley. 1 online resource (325 p.).
5. De Hoffmann, E.Q.H.E. and V.Q.V.Q. Stroobant, *Mass spectrometry : principles and applications*. 3. ed. ed. 2008, 2009, 2011, 2012. 2007, Chichester [u.a.]: Chichester [u.a.] : Wiley. XII, 489 S., Ill., graph. Darst., 25 cm.
6. Horneffer, V., et al., *Is the incorporation of analytes into matrix crystals a prerequisite for matrix-assisted laser desorption/ionization mass spectrometry? A study of five positional isomers of dihydroxybenzoic acid22Dedicated to Professor Michael T. Bowers on the occasion of his 60th birthday.* International Journal of Mass Spectrometry, 1999. **185-187**: p. 859-870.
7. Blincoe, W.D., et al., *Practical guide on MALDI-TOF MS method development for high throughput profiling of pharmaceutically relevant, small molecule chemical reactions.* Tetrahedron, 2020. **76**(36): p. 131434.
8. Byrd, H.C.M. and C.N. McEwen, *The Limitations of MALDI-TOF Mass Spectrometry in the Analysis of Wide Polydisperse Polymers.* Analytical Chemistry, 2000. **72**(19): p. 4568-4576.
9. Wypych, G.Q.G., *Handbook of polymers*. Second edition ed. 2016, Toronto: Toronto : ChemTec Publishing. 1 Online-Ressource (815 Seiten).
10. Tatro, S.R., et al., *Matrix-assisted laser desorption/ionization (MALDI) mass spectrometry: determining Mark–Houwink–Sakurada parameters and analyzing the breadth of polymer molecular weight distributions.* Polymer, 2002. **43**(8): p. 2329-2335.
11. Payne, M.E. and S.M. Grayson, *Characterization of Synthetic Polymers via Matrix Assisted Laser Desorption Ionization Time of Flight (MALDI-TOF) Mass Spectrometry.* J Vis Exp, 2018(136).

12. contriubutors, W. *Polyethylene glycol*. 16.10.2023 [cited 2024 8.01.2024]; Available from: https://en.wikipedia.org/wiki/Polyethylene_glycol.

13. KGaA, M. *Polyethylene Glycol (PEG)Selection Guide*. 2024 [cited 2024 08/01/2024]; Available from: https://www.sigmaaldrich.com/AT/de/technical-documents/technical-article/materials-science-and-engineering/drug-delivery/polyethylene-glycol-selection-guide.

14. contriubutors, W. *Polyimide*. 25.12.2023 [cited 2024 8.01.2024]; Available from: https://en.wikipedia.org/wiki/Polyimide.

15. Omnexus. *Comprehensive Guide on Polyimide (PI)*. 2021 [cited 2024 08.01.2024]; Available from: https://omnexus.specialchem.com/selection-guide/polyimide-pi-plastic.

16. contriubutors, W. *Poly(methyl methacrylate)*. 27.12.2023 [cited 2024 8.01.2024]; Available from: https://en.wikipedia.org/wiki/Poly(methyl_methacrylate).

17. Omnexus. *Comprehensive Guide on Polymethyl methacrylate (PMMA or Acrylic)*. 2021 [cited 2024 08.01.2024]; Available from: https://omnexus.specialchem.com/selection-guide/polymethyl-methacrylate-pmma-acrylic-plastic.

18. Technologies, S. *Know Your Materials: Polymethyl Methacrylate (PMMA/Acrylic)*. 2021 [cited 2024 08.01.2024]; Available from: https://sybridge.com/polymethyl-methacrylate-pmma/.

19. contriubutors, W. *Polystyrene*. 5.01.2024 [cited 2024 8.01.2024]; Available from: https://en.wikipedia.org/wiki/Polystyrene.

20. Encyclopaedia, T.E.o. *polystyrene*. 1998 05.05.2023 [cited 2024 08.01.2024]; Available from: https://www.britannica.com/science/polystyrene.

21. Tesfamariam, W.H. *Polystyrene Uses, Features, Production and Definition*. 2022 [cited 2024 08.01.2024]; Available from: https://www.xometry.com/resources/materials/polystyrene/.

22. contriubutors, W. *Polyvinylpyrrolidone*. 16.12.2023 [cited 2024 8.01.2024]; Available from: https://en.wikipedia.org/wiki/Polyvinylpyrrolidone.

23. Franco, P. and I. De Marco, *The Use of Poly(N-vinyl pyrrolidone) in the Delivery of Drugs: A Review.* Polymers (Basel), 2020. **12**(5).

24. contriubutors, W. *Polyvinyl acetate*. 22.12.2023 [cited 2024 8.01.2024]; Available from: https://en.wikipedia.org/wiki/Polyvinyl_acetate.

25. Encyclopaedia, T.E.o. *polyvinyl acetate*. 1998 29.09.2023 [cited 2024 08.01.2024]; Available from: https://www.britannica.com/science/polyvinyl-acetate.

26. Commerce, U.S.S.o. *NIST Synthetic Polymer MALDI Recipes Database*. 2014 [cited 2024 08.01.2024]; Available from: https://maldi.nist.gov/.

27. Müller, R., et al., *Molecular weight determination of high molecular mass (glyco)proteins using CGE-on-a-chip, planar SDS-PAGE and MALDI-TOF-MS.* ELECTROPHORESIS, 2010. **31**(23-24): p. 3850-3862.

10 Table of figures

11 Table of tables

12 Appendix:

12.1 α-Cyano-4-hydroxycinnamic acid – CHCA

Figure 26: M_n and M_w with CHCA of PEG a) 400 g/mol, b) 600 g/mol, c) 1000 g/mol and d) 2000 g/mol

Figure 27: Mass distributions (width of bar) and maxima (black square) with CHCA of PEG a) 400 g/mol, b) 600 g/mol, c) 1000 g/mol and d) 2000 g/mol
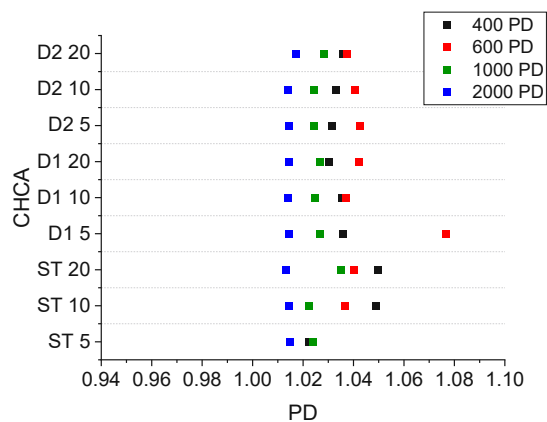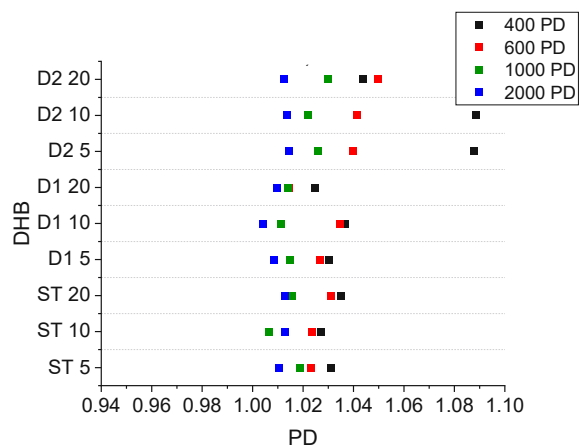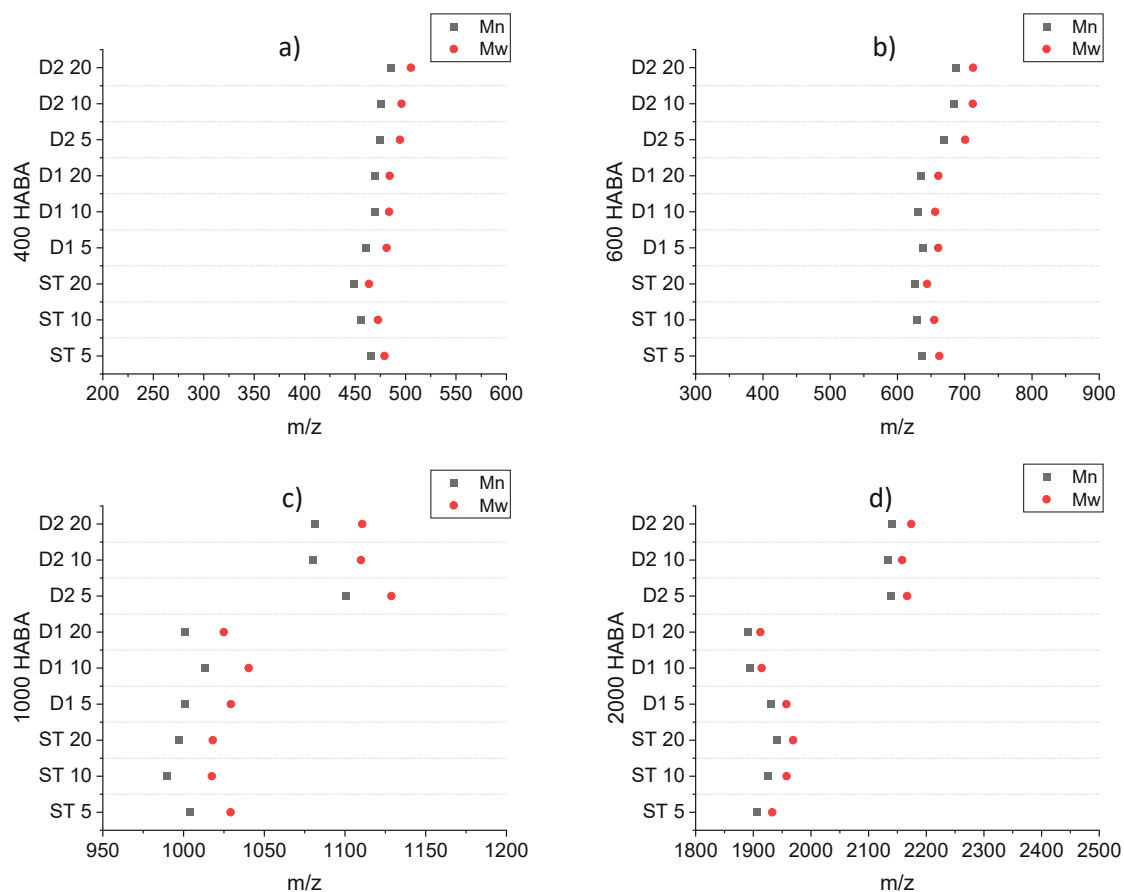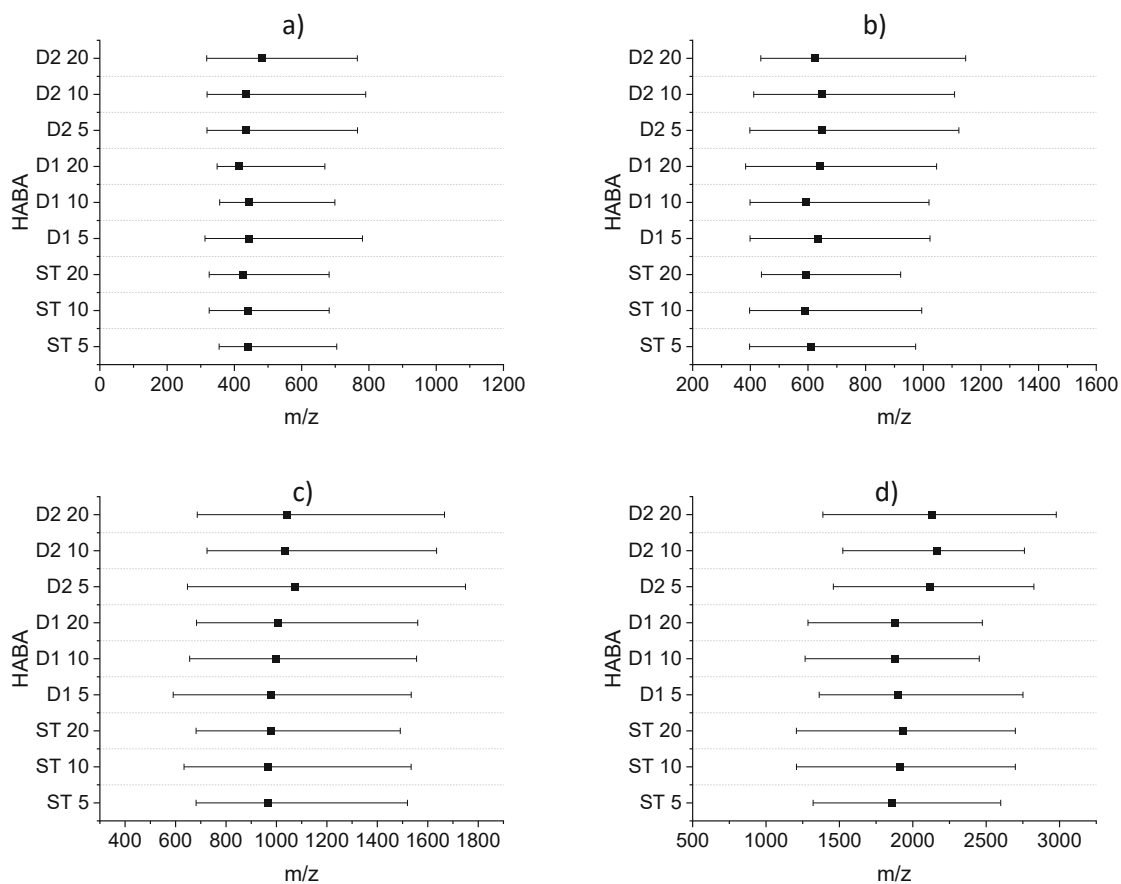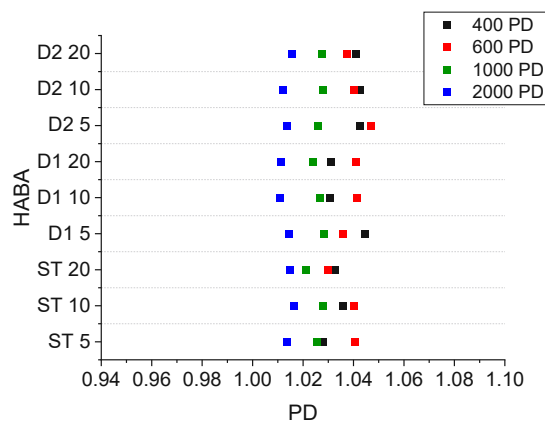

Figure 28: PD of all PEG masses with CHCA

12.2 Trans-2-(3-(4-tert-Butylphenyl)-2-methyl-2-propenyliedene]-malonnitrile – DCTB
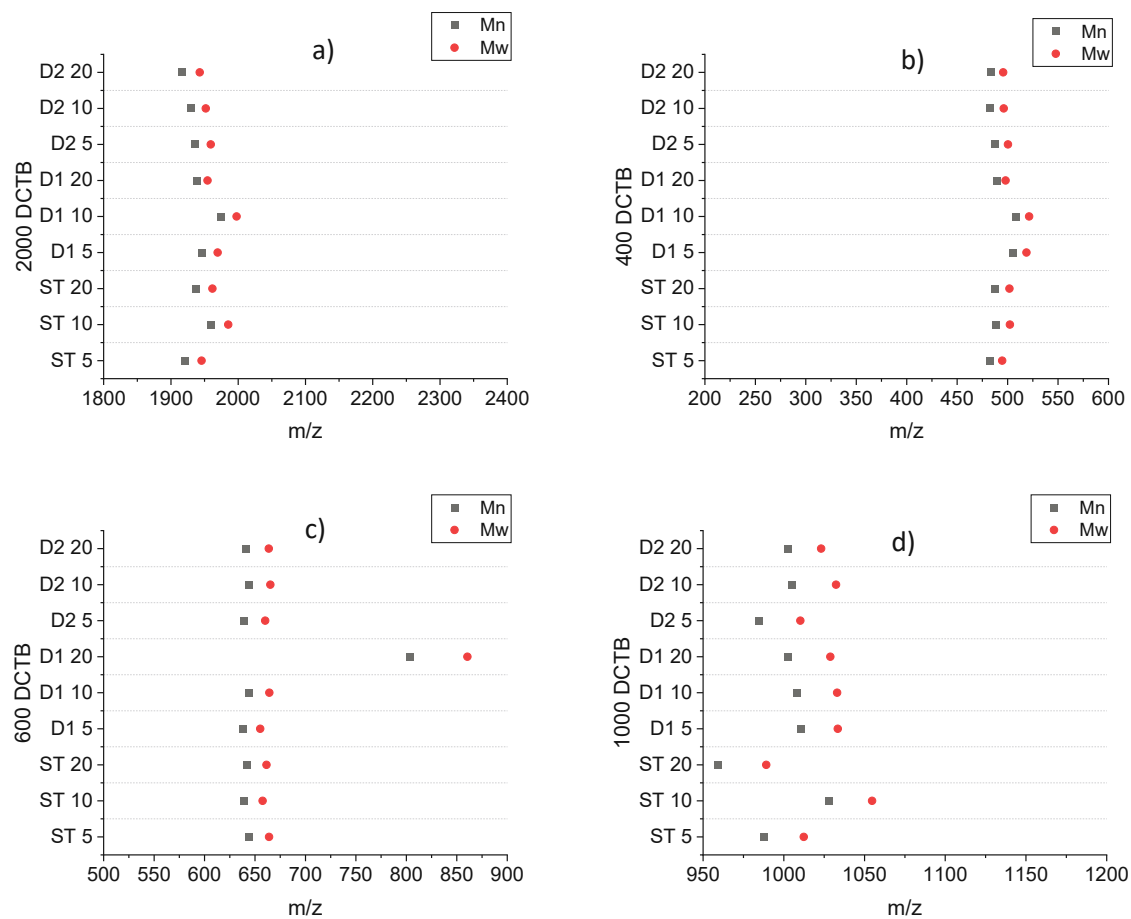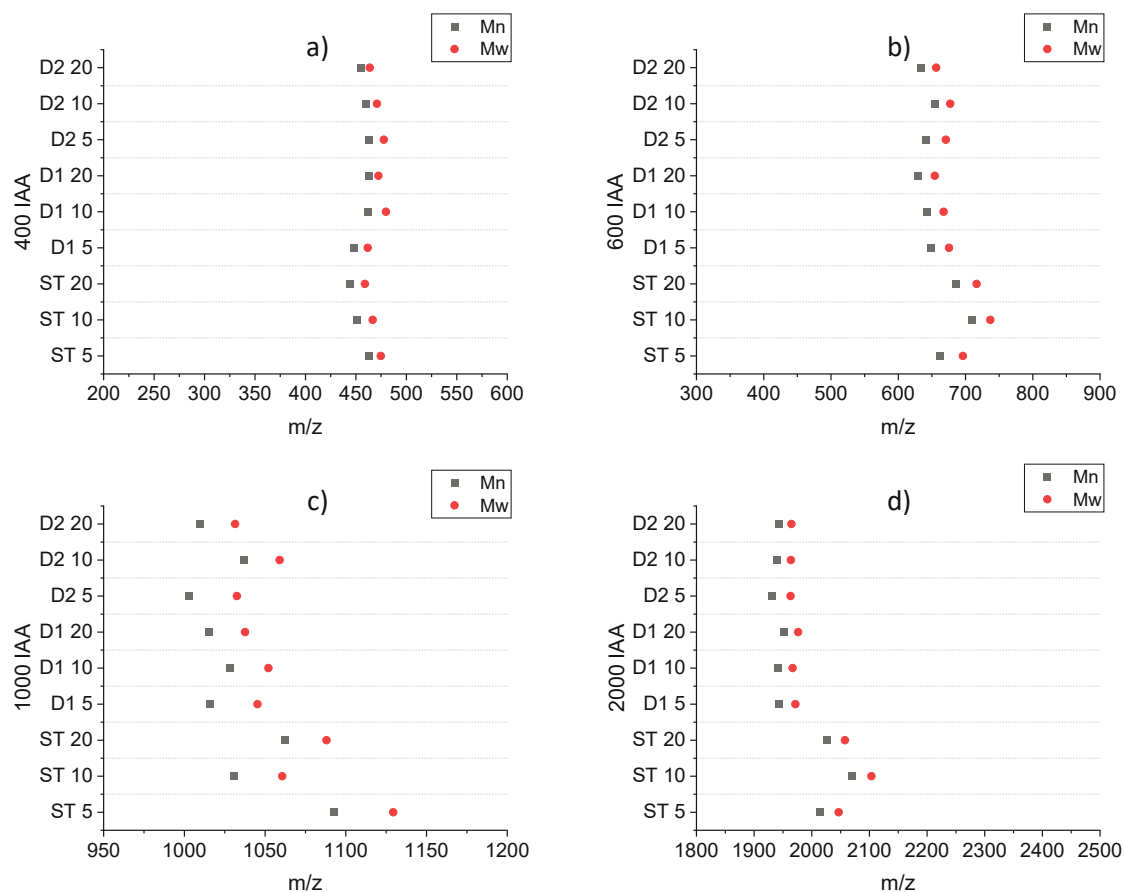

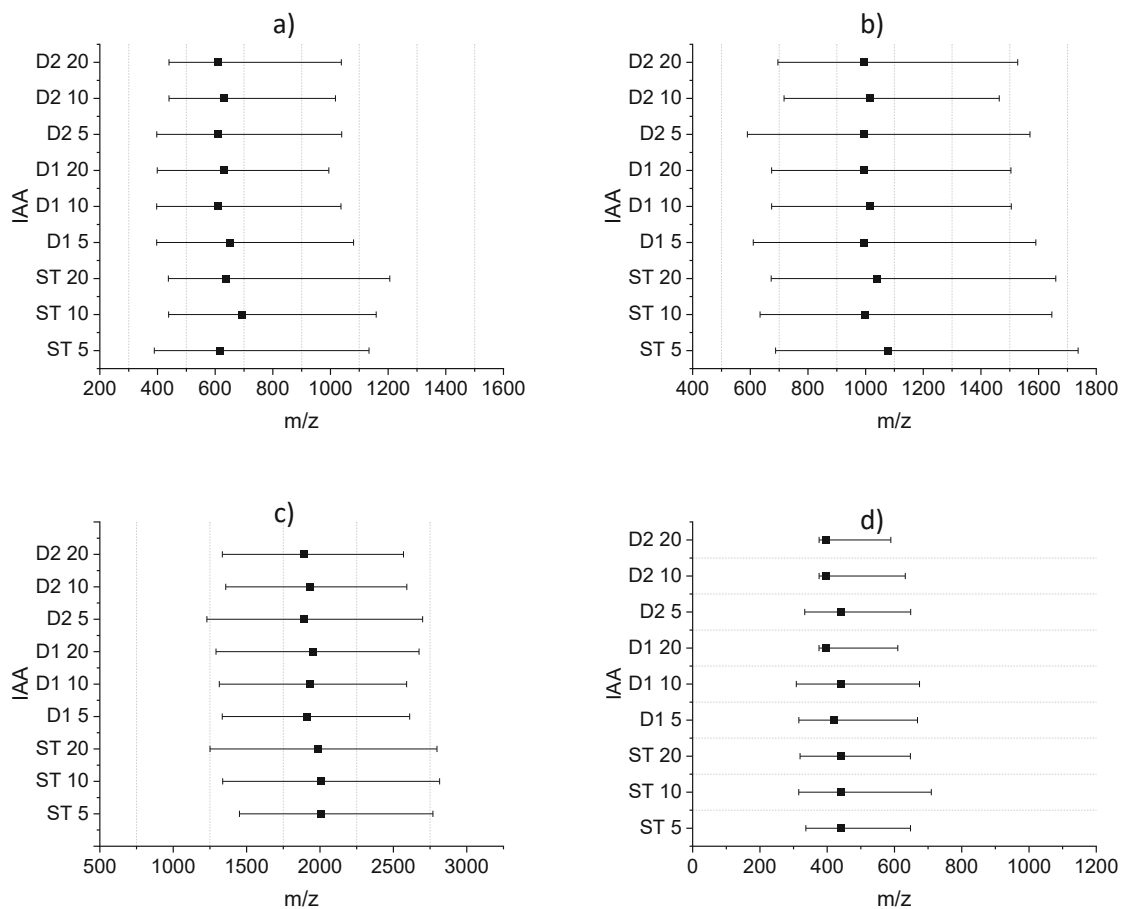*Figure 29: M_n and M_w with DCTB of PEG a) 400 g/mol, b) 600 g/mol, c) 1000 g/mol and d) 2000 g/mol*
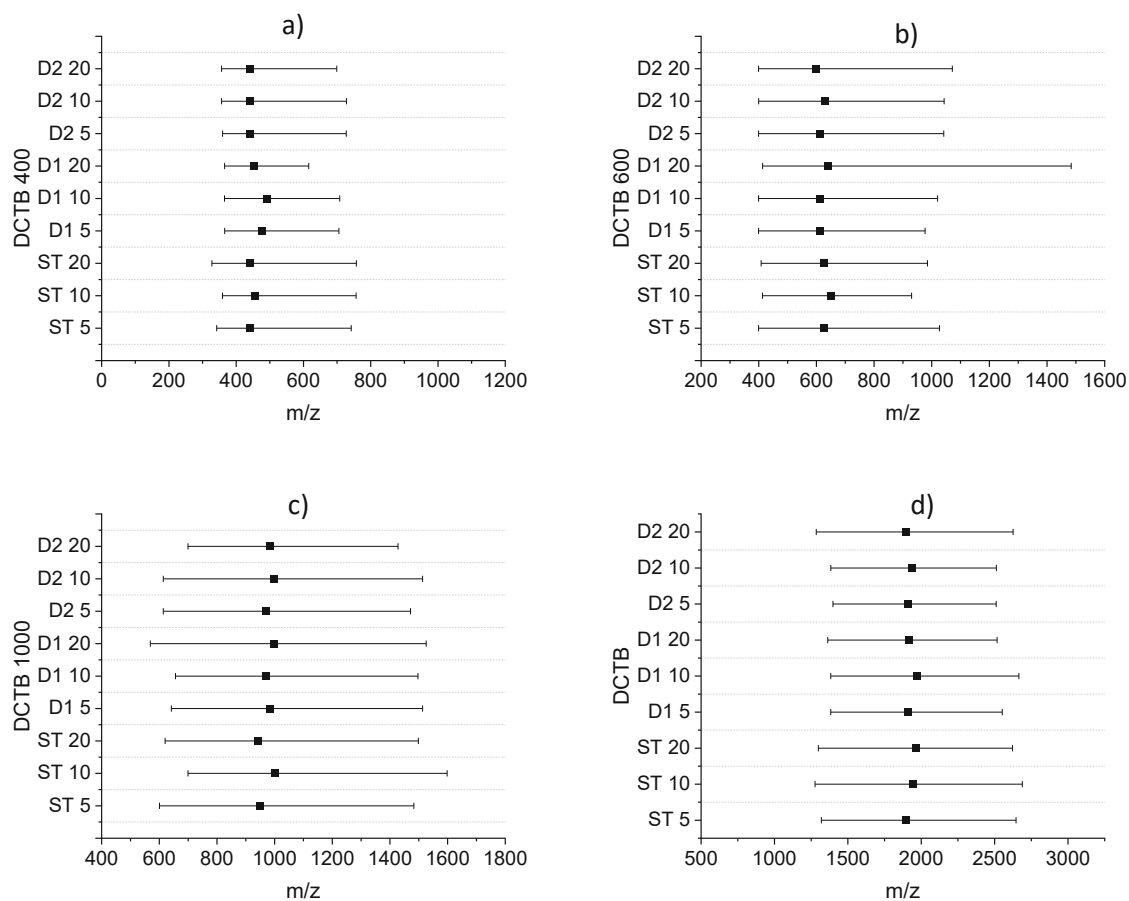
Figure 30: Mass distributions (width of bar) and maxima (black square) with DCTB of PEG a) 400 g/mol, b) 600 g/mol, c) 1000 g/mol and d) 2000 g/mol
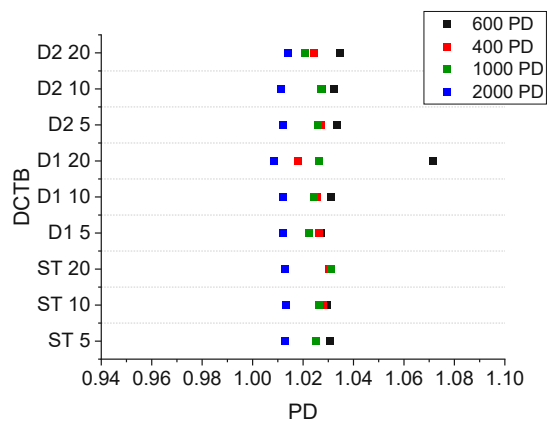
Figure 31: PD of all PEG masses with DCTB

12.3 2,5-Dihydroxybenzoic acid- DHB
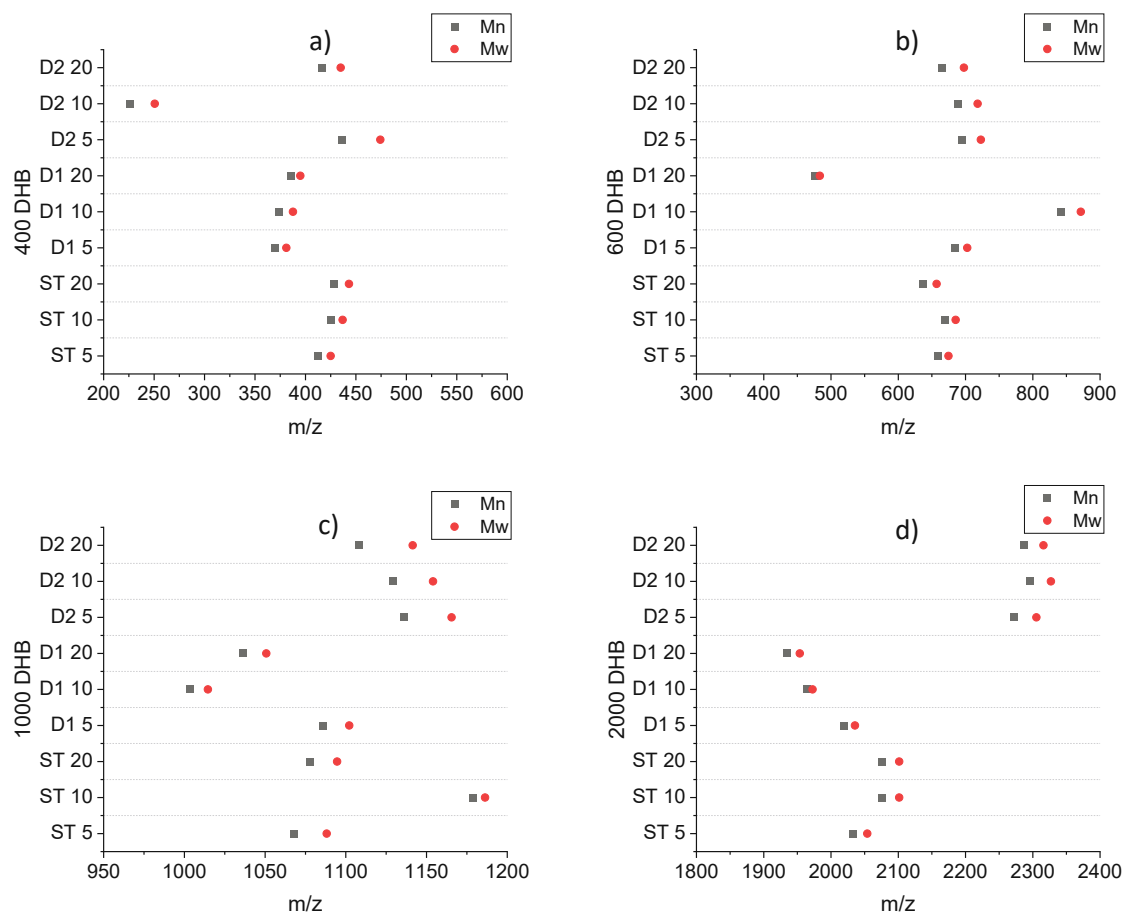
Figure 32: M_n and M_w with DHB of PEG a) 400 g/mol, b) 600 g/mol, c) 1000 g/mol and d) 2000 g/mol
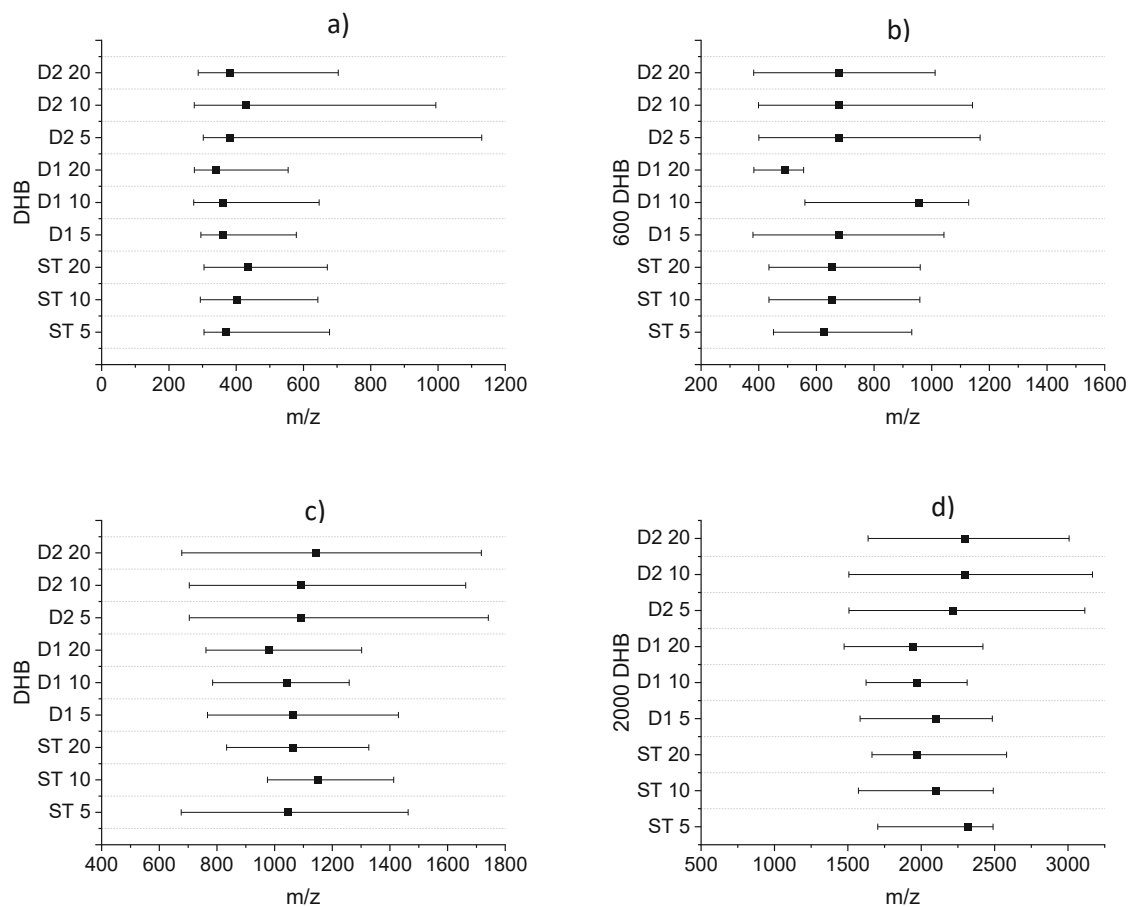
Figure 33: Mass distributions (width of bar) and maxima (black square) with DHB of PEG a) 400 g/mol, b) 600 g/mol, c) 1000 g/mol and d) 2000 g/mol
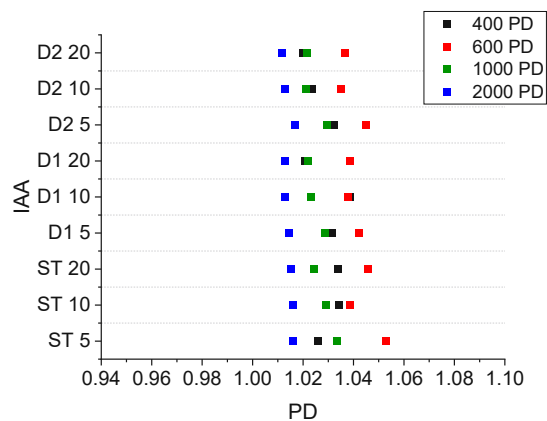

Figure 34: PD of all PEG masses with DHB

## 12.4 2-[(E)-(4-Hydroxyphenyl)diazenyl]benzoic acid- HABA

Figure 35: M_n and M_w with HABA of PEG a) 400 g/mol, b) 600 g/mol, c) 1000 g/mol and d) 2000 g/mol

Figure 36: Mass distributions (width of bar) and maxima (black square) with HABA of PEG a) 400 g/mol, b) 600 g/mol, c) 1000 g/mol and d) 2000 g/mol

Figure 37: PD of all PEG masses with HABA

12.5 Indole-3-acetic acid- IAA

Figure 38: M_n and M_w with IAA of PEG a) 400 g/mol, b) 600 g/mol, c) 1000 g/mol and d) 2000 g/mol

Figure 39: Mass distributions (width of bar) and maxima (black square) with IAA of PEG a) 400 g/mol, b) 600 g/mol, c) 1000 g/mol and d) 2000 g/mol

Figure 40: PD of all PEG masses with IAA

12.6 9H-Pyrido[3,4-b]indol- Nor
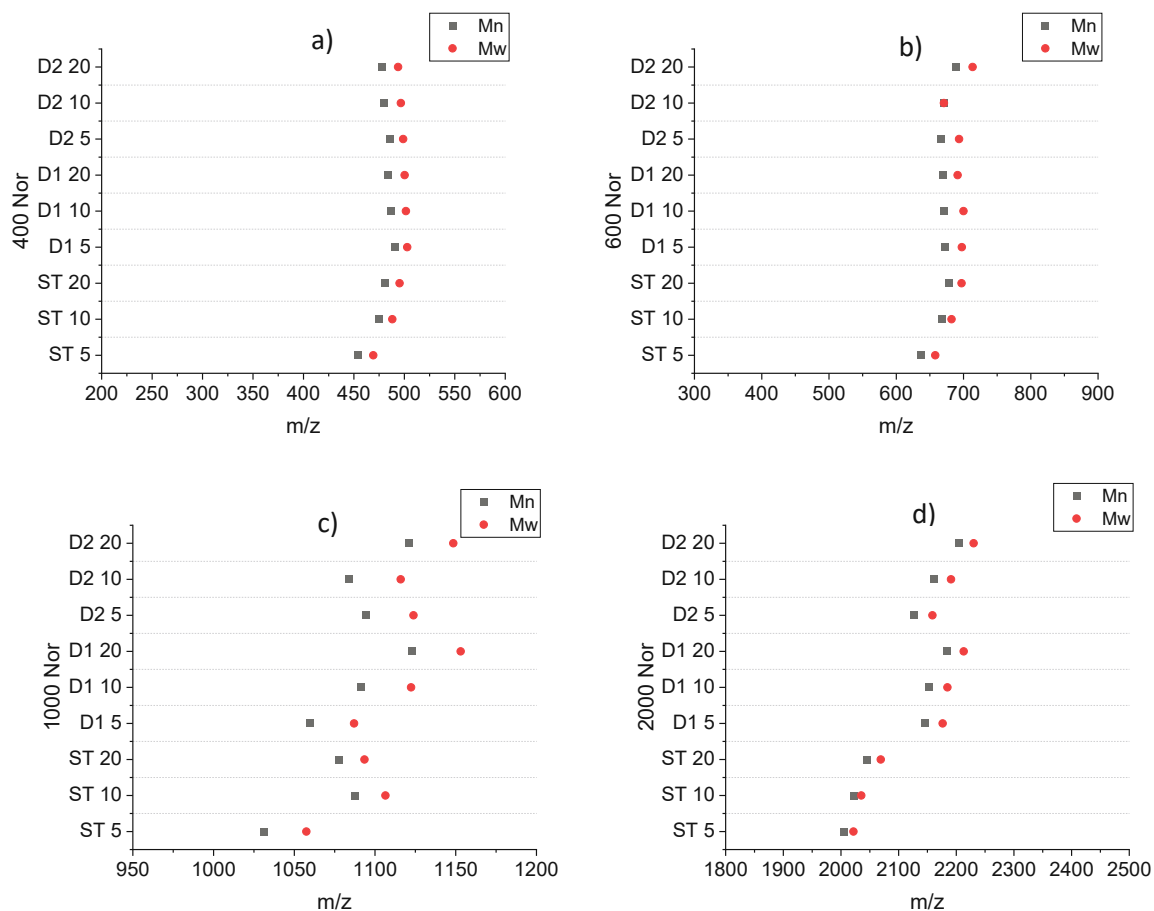
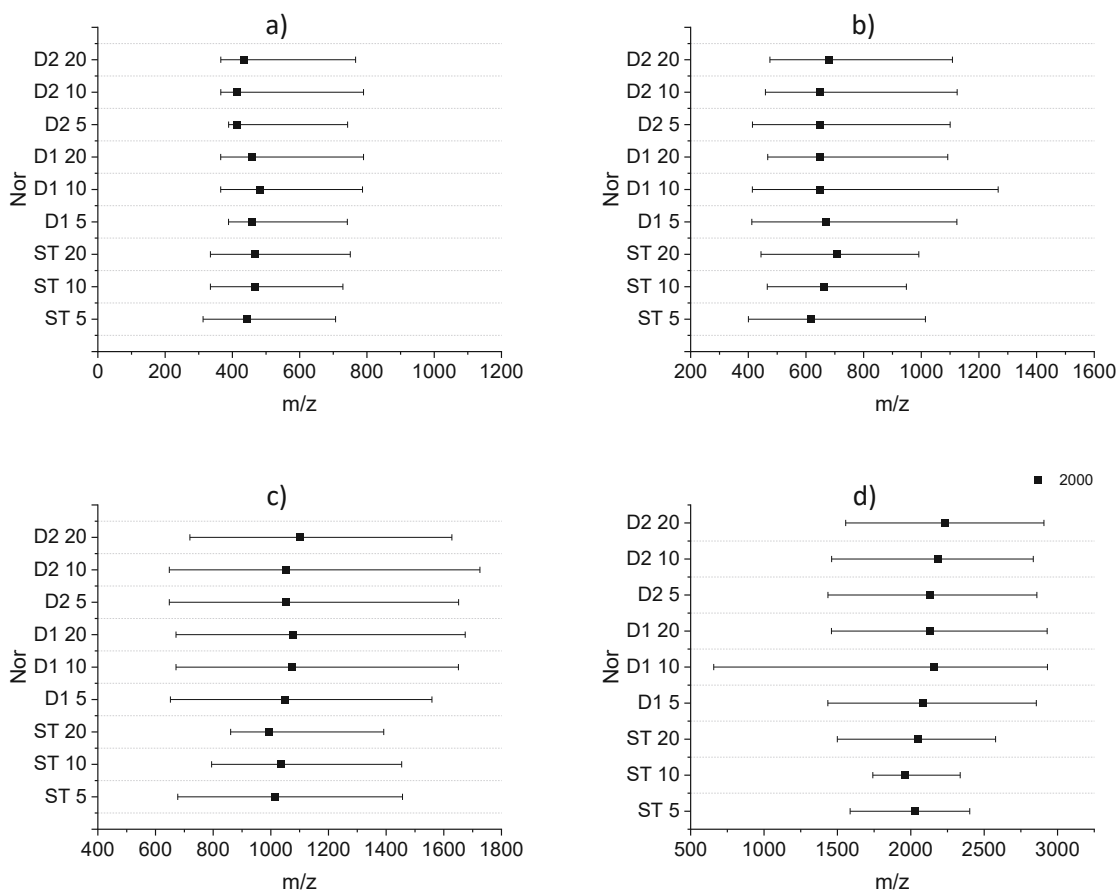*Figure 41: M_n and M_w with Nor of PEG a) 400 g/mol, b) 600 g/mol, c) 1000 g/mol and d) 2000 g/mol*

Figure 42: Mass distributions (width of bar) and maxima (black square) with Nor of PEG a) 400 g/mol, b) 600 g/mol, c) 1000 g/mol and d) 2000 g/mol
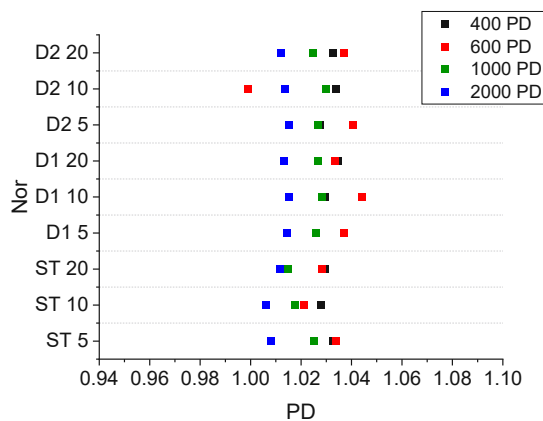

Figure 43: PD of all PEG masses with Nor

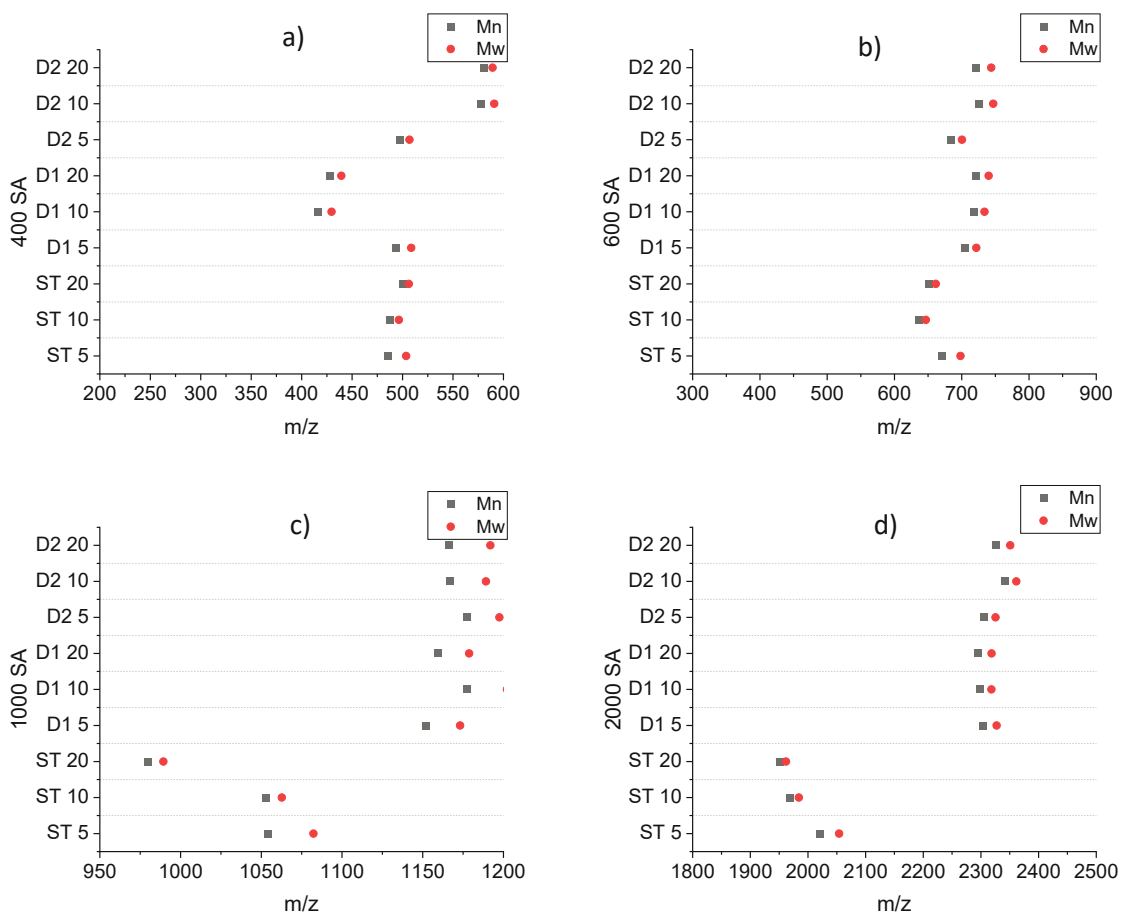## 12.7 3,5 Dimethoxy-4-hydroxycinnaminic (Sinapinic) acid- SA

Figure 44: M_n and M_w with SA of PEG a) 400 g/mol, b) 600 g/mol, c) 1000 g/mol and d) 2000 g/mol
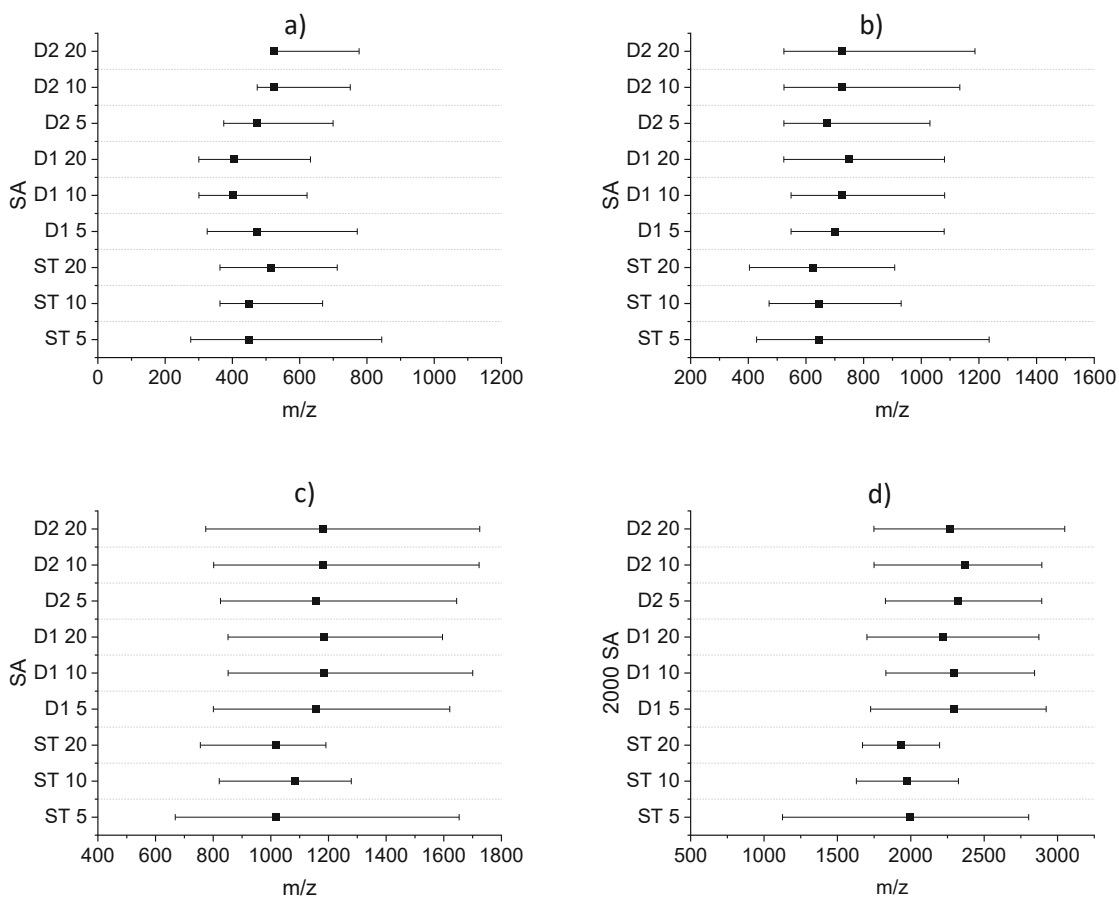
Figure 45: Mass distributions (width of bar) and maxima (black square) with SA of PEG a) 400 g/mol, b) 600 g/mol, c) 1000 g/mol and d) 2000 g/mol
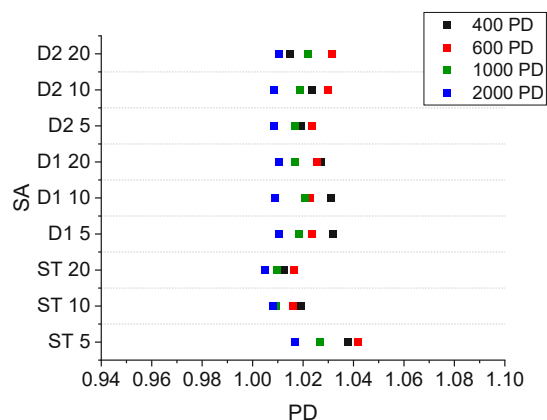

Figure 46: PD of all PEG masses with SA

Supplementary information https://owncloud.tuwien.ac.at/index.php/s/8pkeU5qjz86D65v with password "PEGspectra" or contact untersulzner.v@gmail.com.